AMERICAN UNIVERSITY OF BEIRUT

IDENTIFICATION AND VALIDATION
OF NOTCH2 AS AN INTERACTING PARTNER WITH
THE CARDIOMYOPATHY ASSOCIATED PROTEIN RBM20

by
HOUDA NABIL TANTAWI

A thesis
submitted in partial fulfillment of the requirements
for the degree of Master of Science
to the Department of Biochemistry and Molecular Genetics
of the Faculty of Medicine
at the American University of Beirut
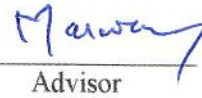
Beirut, Lebanon
June 2020

AMERICAN UNIVERSITY OF BEIRUT

IDENTIFICATION AND VALIDATION OF NOTCH2 AS AN INTERACTING PARTNER WITH THE CARDIOMYOPATHY ASSOCIATED PROTEIN RBM20

by
HOUDA NABIL TANTAWI

Approved by:

_____
Dr. Marwan Refaat, Associate Professor   Advisor
Biochemistry and Molecular Genetics

_____
Dr. Diana Jaalouk, Associate Professor   Member of Committee
Biology

_____
Dr. Ayad A Jaffa, Chairperson and Professor   Member of Committee
Biochemistry and Molecular Genetics

_____
Dr. Georges Nemer, Professor   Member of Committee
Biochemistry and Molecular Genetics

Date of thesis defense: June, 22, 2020

AMERICAN UNIVERSITY OF BEIRUT

THESIS, DISSERTATION, PROJECT RELEASE FORM

Student Name:

__Tantawi_____ __Houda_____ __Nabil_____
Last   First   Middle

☒ Master's Thesis   ○ Master's Project   ○ Doctoral Dissertation

☐   I authorize the American University of Beirut to: (a) reproduce hard or electronic copies of my thesis, dissertation, or project; (b) include such copies in the archives and digital repositories of the University; and (c) make freely available such copies to third parties for research or educational purposes.

☒   I authorize the American University of Beirut, to: (a) reproduce hard or electronic copies of it; (b) include such copies in the archives and digital repositories of the University; and (c) make freely available such copies to third parties for research or educational purposes after:

Three ---- years from the date of submission of my thesis, dissertation, or project.

_____   __July 7, 2020____
Signature   Date

ACKNOWLEDGMENTS

AN ABSTRACT OF THE THESIS OF

Houda Nabil Tantawi   for   Master of Science
                                     Major: Biochemistry

Title: Identification and Validation of Notch2 as an Interacting Partner with the
       Cardiomyopathy Associated Protein RBM20

Background: Mutations in the gene encoding the RNA-binding protein (RBM20) have recently been identified to segregate with aggressive forms of familial dilated cardiomyopathy (DCM). RBM20 has been shown to regulate splicing of over 30 genes, most of which are implicated in ion homeostasis and muscle biology, but not much is known about its interacting partners. Using phage display profiling of the C-terminal fragment of recombinant RBM20, a group in Dr. Jaalouk's lab identified a panel of potential interacting partners for RBM20, including Neurogenic Locus Notch Homolog Protein 2 (Notch2). Mutations in the latter are known to be implicated in the development of cardiomyopathies.

Our objective is to gain a better understanding of the molecular mechanisms by which mutations or down-regulation of the *RBM20* gene lead to the development of the Dilated Cardiomyopathy disease (DCM). To this end, identifying the protein interacting partners of RBM20 protein may provide a better insight into the pathobiology of *RBM20*-mediated DCM.

Aims: In this study, we hypothesize that Notch2 protein interacts with RBM20 and that cardiomyopathies that arise due to mutations in *RBM20* gene are partly mediated by a disruption in the interaction between RBM20 and Notch2 proteins. Thus, we first assessed the expression and the intracellular distribution of Notch2 protein and to determine if it co-localizes with RBM20. Second, we aimed to determine if there is direct interaction between RBM20 and Notch2 proteins.

Methods: For the purpose of studying the sub-cellular distribution and the co-localization between RBM20 and Notch2 proteins, we performed Immunofluorescence (IF) staining assays on Rhabdomyosarcoma (RD) cells. In addition, we performed Western Blotting followed by Co-Immunoprecipitation assays for the assessment of the direct protein-protein interaction between RBM20 and Notch2 proteins in RD cells.

Results: Immunofluorescence staining results revealed an expression of RBM20 proteins in both the cytoplasm and the nucleus of 97.8 % of counted RD cells, yet these proteins were mostly distributed in the nucleus. Similarly, 59.5 % of RD cells expressed Notch2 proteins in both the cytoplasmic and nuclear compartments, yet most of these proteins were localized in the nucleus. In addition, Western Blotting experiments on RD cells showed an expression of Notch2 proteins having a molecular weight of ~ 106 KDa, and two RBM20 protein isoforms, one of ~ 125 KDa and the other of ~ 45 KDa. Finally, our Co-Immunoprecipitation assay suggested a protein-protein interaction between RBM20 and Notch2 proteins, where RBM20 was pulled down by Notch2 and appeared at ~ 129 KDa on the blot probed with RBM20 antibody.

Conclusion: Taken together, our data suggest a possible protein-protein interplay between RBM20 and Notch2 proteins. Additional experiments are needed to validate these findings and to decipher the importance of this interaction for the proper function of RBM20 protein.

CONTENTS

ILLUSTRATIONS

TABLES

ABBREVIATIONS

ARVC/D   Arrhythmogenic right ventricular
                cardiomyopathy/dysplasia

CPVT   Catecholaminergic polymorphic ventricular
                tachycardia

DCM   Dilated Cardiomyopathy

HCM   Hypertrophic Cardiomyopathy

LQTS   Long-QT syndrome

LVNC   left ventricular non-compaction

SQTS   Short-QT syndrome

SUNDS   Sudden unexpected nocturnal death syndrome

RCM   Restrictive Cardiomyopathy

ACM   Arrhythmogenic Cardiomyopathy

LV   Left ventricle

RBM20   RNA-binding protein 20

DSP   Desmoplakin

PLN   Phospholamban

MYBPC3   Myosin binding protein C

TTN   Titin gene

KDa   Kilo Dalton

ZnF   Zinc finger

RRM   RNA recognition motif

RS   Arginine-Serine

RSRSP   Arginine-serine-arginine-serine-proline

RRE   RNA recognition element

SnRNP	Small nuclear ribonucleoproteins
UCUU	Uracil-Cysteine-Uracil-Uracil
CamkIIδ	Ca2+/calmodulin-dependent protein kinase II delta
DST	Dystonin
ENAH	Enabled homolog
IMMT	Inner membrane protein, mitochondrial
LDB3	LIM domain binding 3
LMO7	LIM domain only protein 7
MLIP	Muscular-enriched A-type laminin-interacting protein
LRRFIP1	Leucine-rich repeat (in FLII) interacting protein 1
MYH7	Myosin heavy chain 7
MYOM1	Myomesin 1
NEXN	Nexilin
OBSCN	Obscurin
PDLIM3	PDZ and LIM domain 3
RTN4	Reticulon 4
RyR2	Ryanodine receptor protein 2
SORBS1	Sorbin and SH3 domain containing protein 1
TNNT2	Troponin T type 2
MDa	Mega Dalton
N2BA-G	Giant N2BA titin isoform
Pre-mRNA	Precursor of messenger RNA
FCT	Fetal cardiac titin
LTCC	L-type calcium channel
ER	Endoplasmic reticulum
PCR	Polymerase chain reaction

C-RBM20	C-terminal fragment of RBM20 protein
NOTCH	Neurogenic locus notch homolog protein
NECD	Notch extracellular domain
EGFR	Epidermal growth factor-like repeats
NRR	Negative regulatory region
NICD	Notch intracellular domain
RAM	RBP-Jk associated molecular domain
ANK	Ankyrin/cdc 10 repeats
NLS	Nuclear localization signals
PEST	Proline-Glutamic acid-Serine-Threonine
PM	Plasma membrane
TMD	Transmembrane domain
OPA	Opa repeats
TAD	Transactivation domain
LIN	LIN12/Notch repeats
DSL	Delta-Serrate-Lag2 domain
EGF	Epidermal growth factor
CR	cysteine rich region
ADAM	A disintegrin and metalloproteinase
PEN2	Presenilin enhancer 2
APH1	Anterior pharynx-defective 1
CSL	C promoter-binding factor in humans, Suppressor of hairless in Drosophila, LAG
MAML1	Mastermind-like transcriptional co-activator 1
EMT	Epithelial-to-mesenchymal transition
Jag1	Jagged 1

Jag2	Jagged 2
PSEN1	Presenilin 1
PSEN2	Presenilin 2
PLA	Proximity ligation assay
RD	Rhabdomyosarcoma
ATCC	American Type Culture Collection
MEFs	Mouse embyo fibroblast
DMEM	Dulbecco's Modified Eagle's Medium
FBS	Fetal bovine serum
PBS	Phosphate buffered saline
IF	Immunofluorescence staining
PFA	Paraformaldehyde
BSA	Bovine Serum Albumin
DAPI	4',6-diamidino-2 phenylindole
RIPA buffer	Radioimmunoprecipitation assay buffer
ddH2O	Double distilled water
SDS-PAGE	Sodium Dodecyl Sulfate-Polyacrylamide Gel Electrophoresis
SDS	Sodium Dodecyl Sulfate
TCA	Trichloroacetic acid
TBS-T	Tris buffered saline with tween
Tween20	Polyoxyethylene sorbitol ester
HRP	Horseradish peroxidase
PMSF	Phenylmethylsulfonyl fluoride
LWB	Last wash buffer
EB	Elution buffer

Co-IP	Co-immunoprecipitation
IP	Immunoprecipitation
IB	Immunoblot
PLA	Proximity Ligation Assay
P13-k	Phosphoinositide 3-kinase

CHAPTER I

LITERATURE REVIEW

A. Cardiomyopathies

1. Definition

Cardiomyopathies refer to a group of heterogeneous intrinsic diseases of the myocardium with structural and functional abnormalities in the absence of coronary disease, hypertension, valvular disease, or congenital malformation sufficient to explain them. They are defined as unfavorable conditions that predispose to impaired myocardial contraction, and diastolic dysfunction denoted by defective ventricular filling [1, 2]. In 2006, the American Heart Association defined cardiomyopathies as following: *"Cardiomyopathies are a heterogeneous group of diseases of the myocardium associated with mechanical and/or electrical dysfunction that usually (but not invariably) exhibit inappropriate ventricular hypertrophy or dilatation and are due to a variety of causes that frequently are genetic. Cardiomyopathies either are confined to the heart or are part of generalized systemic disorders"* [3]. In most cases, Cardiomyopathy leads to an enlarged, thick, or rigid myocardium. It also might lead in rare cases to the replacement of the diseased myocardium with scar tissue. As Cardiomyopathy worsens, the heart becomes weaker, leading ultimately to heart failure and subsequent inadequate perfusion of tissues, fluid accumulation, and cardiac rhythm dysfunction [4].

2. *Classification*

The American Heart Association (AHA) classifies cardiomyopathies as primary or secondary. In primary cardiomyopathies, the disease process is solely confined to the heart; whereas in secondary cardiomyopathies, the cardiac involvement occurs as part of a systemic condition such as Diabetes Mellitus, Rheumatoid Arthritis, and Emery-Dreifuss muscular dystrophy [3] Primary cardiomyopathies are further classified as genetic, acquired, or mixed in etiology. Genetic cardiomyopathies are caused by chromosomal abnormalities affecting the heart. Acquired cardiomyopathies occur when non-genetic causes lead solely to cardiac complications. Finally, mixed cardiomyopathies are when a common phenotype is eased by genetic and non-genetic means [3, 4].
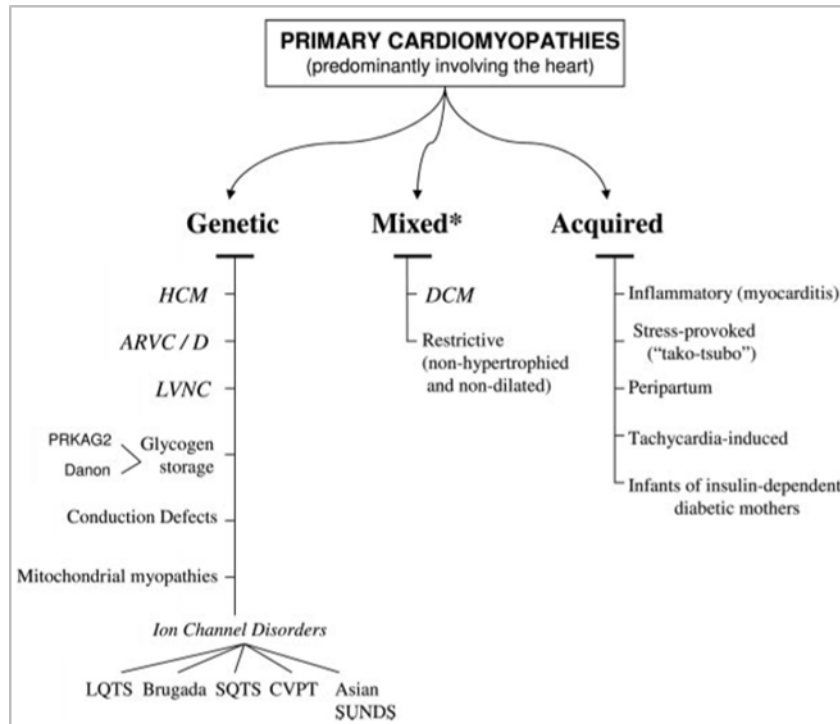
Figure 1 | American Heart Association classification of cardiomyopathies. Abbreviations: **ARVC/D**: arrhythmogenic right ventricular cardiomyopathy/dysplasia; **CPVT**: catecholaminergic polymorphic ventricular tachycardia; **DCM**: dilated Cardiomyopathy; **HCM**: hypertrophic Cardiomyopathy; **LQTS**: long-QT syndrome; **LVNC**: left ventricular non-compaction; **SQTS**: short-QT syndrome; and **SUNDS**: sudden unexpected nocturnal death syndrome [3].

3. *Types*

Primary Cardiomyopathies are usually divided into five main subtypes: Dilated Cardiomyopathy (DCM), Hypertrophic Cardiomyopathy (HCM), Restrictive Cardiomyopathy (RCM), Arrhythmogenic Cardiomyopathy (ACM), Left Ventricular Non-compaction Cardiomyopathy (LVNC) as well as other non-classified subtypes [2].

Dilated Cardiomyopathy is characterized by enlargement of one or both ventricles, normal left ventricular wall thickness, accompanied by systolic and diastolic contractile dysfunction and symptoms of heart failure. It is the most common form of

cardiomyopathies with a prevalence of 1:2500 to 1:250. Additionally, it is one of the leading causes of heart failure and the most frequent cause of heart transplantation. DCM can be familial (in 25% to 35% of cases), inherited primarily in an autosomal dominant manner. Similarly, it can result from a host of environmental, infectious and systemic factors such as alcohol, chemotherapy, and inflammation [3-6].

Hypertrophic Cardiomyopathy is a relatively common form of hereditary heart muscle disease occurring in a prevalence of 1:500 [7]. HCM is characterized by a hypertrophied and non-dilated left ventricle, accompanied by a diminishment of this cavity's dimensions, normal or enhanced contractile function, and impaired ventricular relaxation [8]. It is classified as primary Cardiomyopathy that is caused by autosomal dominant mutations of genes encoding sarcomere proteins [4].

Restrictive Cardiomyopathy (RCM) is a rare type of Cardiomyopathy that is characterized by a normal biventricular chamber size, a normal systolic function, and an increased myocardial stiffness leading to diastolic dysfunction and impaired ventricular filling. RCM can be either primary or secondary. Common causes of RCM include amyloidosis, sarcoidosis, radiation therapy, and scleroderma [4, 9].

Arrhythmogenic Cardiomyopathy (ACM) is an inherited disease of desmosomal proteins in most cases. It is characterized by a progressive loss of the ventricular myocardium and its replacement with fibrofatty tissue leading to palpitations, syncope, arrhythmias, and sudden cardiac death. Right ventricular involvement refers to the classical type of ACM, however, left ventricular and bi-ventricular involvement is recently recognized. ACM has a prevalence of 1:1000 to 5000, and it presents most commonly in people between the second and fourth decade of life. ACM is also

considered one of the leading causes of arrhythmic cardiac arrest in young people and athletes [4, 10-12].

Finally, Left Ventricular Non-compaction (LVNC), also named Spongiform Cardiomyopathy is a very rare genetic cardiomyopathy with a prevalence of 0.05 % to 0.24 %. It is characterized by the presence of prominent tuberculae in the left ventricle, a thin compacted layer, and deep intertrabecular recesses. LVNC is considered a developmental disorder involving failure of compaction of loose myocardial meshwork during fetal organogenesis. Although non-compaction usually affects the left ventricle, but it may also involve the right ventricle. LVNC can be associated with left ventricular dilation, hypertrophy, or other forms of congenital heart disease [13-15].

B. Dilated Cardiomyopathy

1. Definition and pathobiology

Dilated Cardiomyopathy (DCM) is a disease of the myocardium with structural and functional abnormalities. It is defined by dilation of the left ventricle or both ventricles, impaired systolic function, and normal left ventricular (LV) wall thickness in the absence of other cardiac diseases explaining them, such as ischemic coronary artery disease, abnormal pressure, and abnormal volume loading … Despite being a relatively rare disease, it represents a serious health burden affecting both adults and children, as it leads to heart failure, progressive decline in the LV contractile function, arrhythmias, thromboembolism, and sudden cardiac death. Diagnosis is usually made using 2-dimensional echocardiography. Unfortunately, most DCM patients are symptomatic at

the time of diagnosis; however, asymptomatic patients can be identified through
screening of family members of affected patients [3, 4, 16].
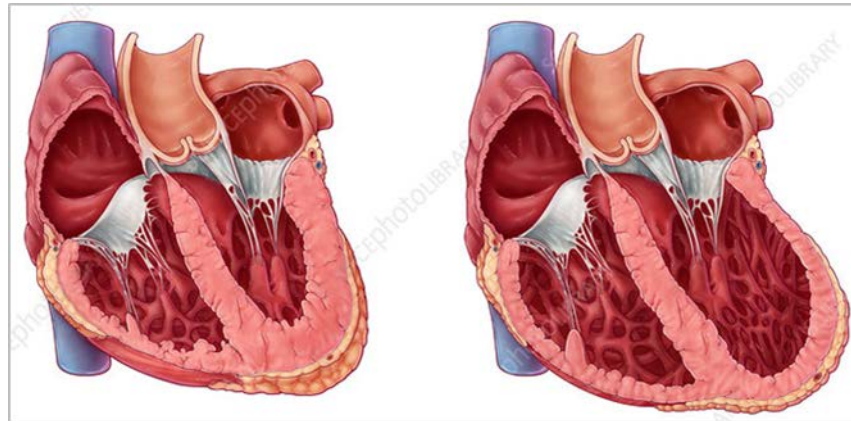
Figure 2 | Dilated Cardiomyopathy. Schematic showing the normal heart (left) and the
diseased heart (right) where the left ventricle is dilated. (www.sciencephoto.com)

2. *Epidemiology*

Dilated Cardiomyopathy is the most common type of cardiomyopathies, yet its
exact prevalence is unknown. However, it is assumed to have a prevalence of 1:2,500
individuals to 1:250 and an incidence of 7 cases per 100,000 individuals. Also, DCM
accounts for 60% of pediatric cardiomyopathies manifesting at the highest rate during
the first year of age [16-18]. DCM is also considered the second most common cause of
heart failure (after coronary artery disease), underlying approx. 36% of all heart failure
cases [19]. Subsequently, DCM is the most common etiology of heart transplantation,
with an estimated prevalence of 40 in 100,000 individuals [20]. DCM can occur in
young children as well as in the elderly; nevertheless, it usually manifests in the third or
fourth decade of life. However, elderly patients are expected to have a worse prognosis
as age is considered a risk factor for mortality in patients with DCM [18]. Moreover, the
relative risk of developing congestive heart failure and mortality is about 30% higher in

black than white individuals. Also, men have a higher risk of having DCM than women, and they even tend to have worse outcomes [21].

3. Etiology

DCM is classified as mixed cardiomyopathy since it can be caused by either genetic or acquired stimuli. However, although different causes of DCM have been identified, many cases remain idiopathic. Examples of acquired causes include infectious agents, toxins, alcohol, chemotherapeutic agents, metals, nutritional deficiency, autoimmune, metabolic, and endocrine disorders [3, 16, 22]. As for the genetic causes, DCM is considered genetically heterogeneous, where mutations in more than 60 genes with more than 400 pathogenic variants have been identified. These genes encode proteins of broad cellular functions, including cytoskeletal, sarcomeric, desmosomal, nuclear, Ca^{2+}-regulating, mitochondrial, ion-channel, and nuclear membrane proteins [16, 23].
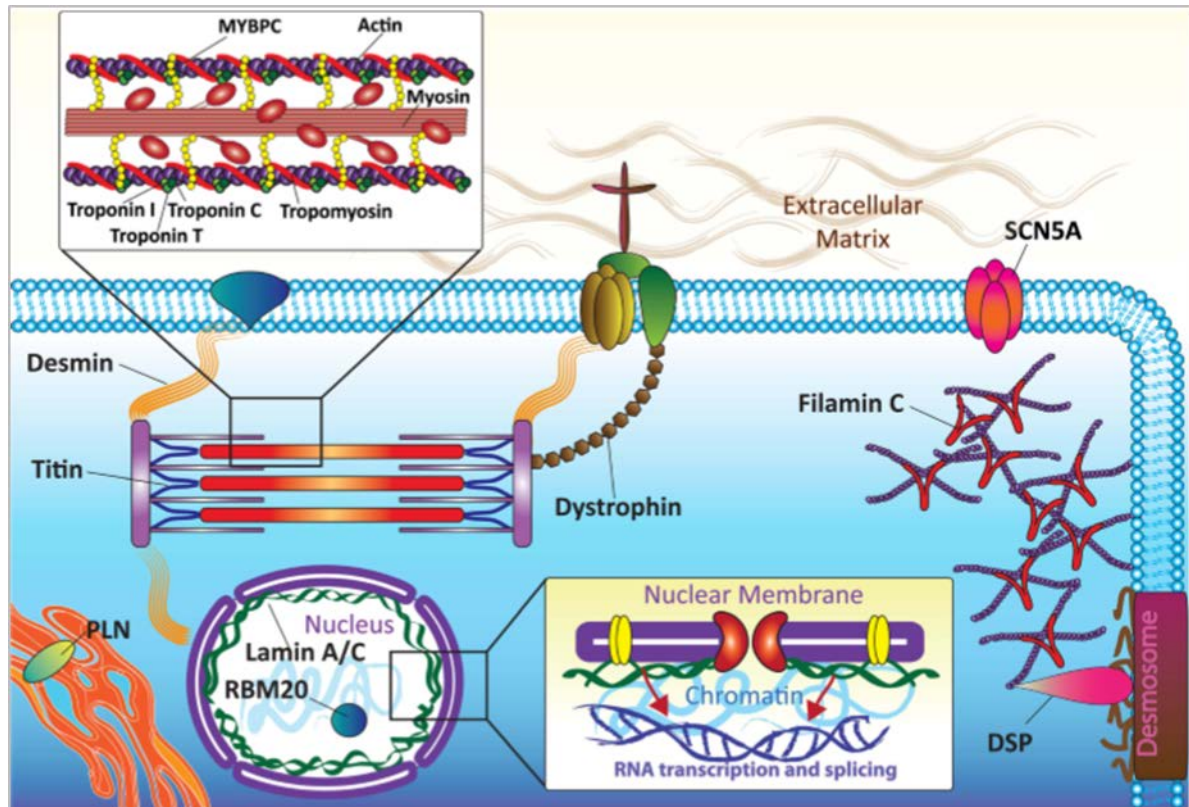
Figure 3 | Drawing of cardiomyocyte indicating the different proteins and genes associated with DCM, and their localization. Abbreviations: **RBM20**: RNA-binding protein 20, **DSP**: desmoplakin, **PLN**: phospholamban, **MYBPC3**: myosin binding protein C [5].

a. The genetic basis of DCM

Approximately 25% to 35% of idiopathic DCM cases are familial and are caused by genetic cues [4]. The different modes of inheritance for familial DCM include autosomal dominant, autosomal recessive, X-linked recessive, and mitochondrial inheritance. However, autosomal dominant mutations, with reduced penetrance and variable expressivity, are the most common mode of inheritance [24]. Table 1 details the top ten genes that are most commonly associated with DCM, their subcellular localization, and prevalence in DCM [19]. Mutations in these genes include missense/nonsense mutations, deletions, insertions, as well as splicing mutations [16,

24]. The pathogenicity arising from the variants of these genes' mutations occurs through dominant-negative effects of abnormal normal-sized proteins or haploinsufficient effects of truncated proteins [16].

TTN truncating mutations are the most common cause of DCM, accounting for ~25% of DCM cases and ~18% of idiopathic cases. *TTN* gene encodes the titin, a giant sarcomeric protein including more than 35,000 amino acids that spans the length of half the sarcomere and acts as a stretch sensor that transmits signals from its anchor, present at the Z band, to its carboxyterminal domain. It is considered a molecular spring regulating and transmitting information about the sarcomere length to both the sarcomere and the cardiomyocyte, thus defining the passive stiffness of the cardiomyocyte [16, 21, 24, 25]. The titin pre-mRNA undergoes extensive alternative splicing, which leads to different titin isoforms that are tissue-specific and developmentally regulated [26].

The *RBM20* gene, which encodes the splicing regulator RNA Binding Motif Protein 20, has been first identified as DCM-associated gene in 2009 [27]. Genetic abnormalities in *RBM20* account for 2% to 5% of DCM cases [27]. Recently, RBM20 protein has been identified as a crucial regulator of the alternative splicing of *TTN* gene [28]. However, the exact mode of action of this protein and its role in the pathophysiology of DCM is still unclear. Other common pathogenic variants, leading to the development of DCM are desmosomal, nuclear, Z-disk, and ion channel genes [19].

Gene (protein)	Protein function	Estimated prevalence in DCM (%)	Age of onset of DCM (years)	Associated disorders	Notes
TTN (titin)	Sarcomere, structural	12-25%	Usually 40-59	Usually isolated DCM	More common in women than in men; variable prognosis but family clustering
LMNA (lamin A/C)	Nuclear membrane	4-6 (up to 30 if conduction disease also present)	30-49; conduction disease usually prominent	Subset of Emery-Dreifuss muscular dystrophy	Most conduction disease cases symptomatic over time; ventricular arrhythmias common
MYH7 (β-myosin heavy chain)	Sarcomere	4-10	Variable: adolescence to 49	Primarily HCM; also LVNC and RCM	Prognosis variable depending on site of genetic variant; homogeneity within families
MYH6 (α-myosin heavy chain)	Sarcomere	4	Variable: adolescence to 49	Primarily HCM	Prognosis variable depending on site of genetic variant; homogeneity within families
MYPN (myopalladin)	Sarcomere, Z-disk	3-4	Variable: adolescence to 59	Usually isolated DCM	Variable presentation with some early deaths due to heart failure
DSP (desmoplakin)	Desmosome	3-4	40-49	ARVC	Identified in multiple patients with advanced DCM although natural history uncertain; arrhythmic burden seems to be much lower than in ARVC
RBM20 (RNA-binding protein 20)	RNA-binding protein, spliceosome	2-5	Adolescence to 39; can present with SCD or advanced heart failure	Usually isolated DCM	Rapid progression: SCD and end-stage heart failure are common, with a high incidence of ventricular arrhythmias
TNNT2 (cardiac muscle troponin T)	Sarcomere	2-3	Variable: adolescence to 49	HCM, LVNC, and RCM	Prognosis variable depending on site of genetic variant; homogeneity within families
SCN5A (sodium channel protein type 5, α subunit)	Ion channel	2-3	Adolescence	Brugada syndrome and LQTS	Early onset, commonly with atrial fibrillation; not associated with risk of ventricular arrhythmias
TPM1 (α-tropomyosin)	Sarcomere	0.5-1.0	Variable: adolescence to 49	HCM, LVNC and RCM	Prognosis variable depending on site of genetic variant; homogeneity within families

Table 1 | Top ten genes in which mutations lead to the development of DCM. [19].

C. RBM20 gene:

1. Structure of RBM20

RBM20 is an RNA-binding protein specific to vertebrate that regulates alternative mRNA splicing. It is predominantly expressed in the striated muscle, with the highest expression levels in the heart [26, 28, 29]. The human *RBM20* gene is located on Chromosome 10 and contains 14 exons. The corresponding RBM20 protein consists of 1,227 amino acids, which makes it relatively large for a splicing regulator. It has a molecular weight of 134.4 KDa and contains six evolutionarily conserved domains, among them are: two Zinc finger (ZnF) domains, one <u>R</u>NA <u>R</u>ecognition <u>M</u>otif (RRM) in exons 6 and 7 which is an RNA-binding domain, and an Arginine-Serine rich (RS) region located in exon 9, that modulates the binding and assembly of the spliceosome complex, and thus it determinates the differential inclusion of exons in the mature mRNA transcript of the target gene [16, 26, 28]. (Figure 4)
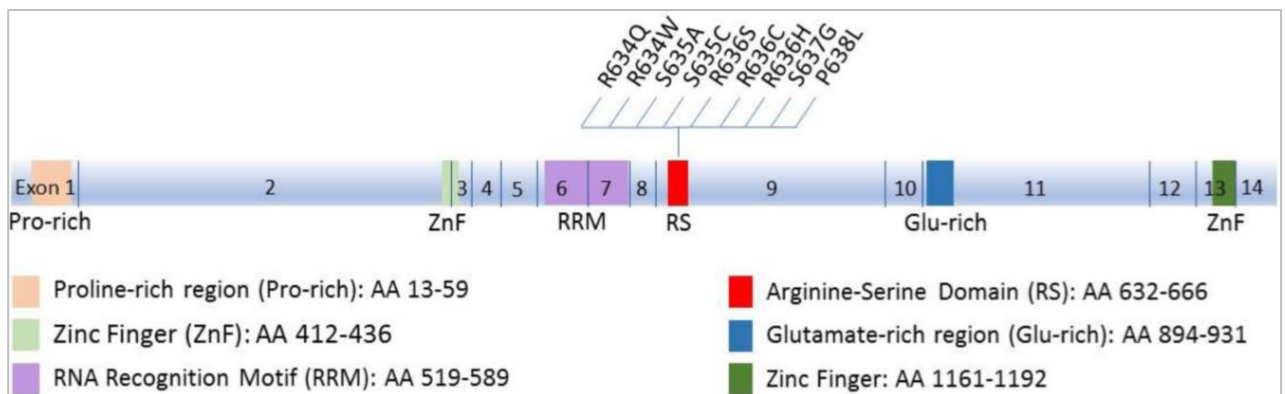
Figure 4 | Schematic diagram showing *RBM20* structure. The 14 exons and functional domains of RBM20 protein are also shown, along with the amino acid residues spanned by these domains. All known mutations in the RS domain are indicated [16].

2. RBM20 mutations in DCM patients

In recent studies, mutations in the *RBM20* gene have been identified as a cause of DCM disease, where *RBM20* ranked among the most common genes linked to this disease [16, 27, 30, 31]. *RBM20* gene deregulation induces aggressive types of DCM: it is associated with young age at diagnosis of DCM, rapid progression towards advanced heart failure, high risk for arrhythmias, high mortality rate, and leads to the youngest mean age for heart transplantation (mean age: 28.5 years) [5, 16, 27, 32].

The most common mutations in *RBM20* gene identified in familial as well as sporadic DCM cases are listed in Table 2 [26]. This list clearly shows that almost all *RBM20* mutations are heterozygous missense mutations and that most of them occur in a 5-amino acid hot spot composed of an arginine-serine-arginine-serine-proline (RSRSP) stretch comprised of the residues 634, 635, 636, 637, and 638 amino acids in the RS domain of the protein [26].

References	Domain	Mutation	Origin	Type	Effect on RBM20	Splicing regulation
Brauch et al, 2009	**RS-rich**	**R634Q**	Familial	Hetero	Unknown	Defective
		R636S	Familial	Hetero	Unknown	Defective
		R636H	Familial	Hetero	Unknown	Unknown
		S637G	Familial	Hetero	Unknown	Defective
		P638L	Familial	Hetero	Unknown	Defective
Li et al, 2010	RRM	V535I	Sporadic	Hetero	Unknown	Unaffected
	RS-rich	**R634Q**	Sporadic	Hetero	Unknown	Defective
		R634W	Familial	Hetero	Exclusion from nucleus	Defective
		R636C	Familial	Hetero	Unknown	Unknown
		R636H	Familial	Hetero	Unknown	Unknown
	Others	R716Q	Familial	Hetero	Unknown	Defective
Millat et al, 2011	**RS-rich**	S637G	Familial	Hetero	Unknown	Unknown
Refaat et al, 2012	L-rich	L83I	Sporadic	Hetero	Unknown	Unknown
	RS-rich	**P638L**	Sporadic	Hetero	Unknown	Defective
	E-rich	D888N	Sporadic	Hetero	Unaffected	Unknown
	Others	S455L	Sporadic	Hetero	Unknown	Unknown
		R703S	Sporadic	Hetero	Unknown	Unknown
		G1031X	Sporadic	Hetero	Unaffected	Effective
		P1081R	Sporadic	Hetero	Unaffected	Unknown
		E1206K	Sporadic	Hetero	Unaffected	Unknown
Guo et al, 2012	**RS-rich**	**S635A**	Sporadic	Hetero	Exclusion from nucleus	Defective Unknown
Wells et al, 2013	**RS-rich**	**R636H**	Familial	Hetero	Unknown	Unknown
Chami et al, 2014	**RS-rich**	**R636H**	Familial	Hetero	Unknown	Unknown
Zhao et al, 2015	Others	R1182H	Unknown	Hetero	Unknown	Unknown
Beqqali et al, 2016	E-rich	E913K	Familial	Hetero	Protein destabilization	Defective
Murayama et al, 2018	**RS-rich**	**R634W**	Familial	Hetero	Exclusion from nucleus	Defective
	Others	G1031X	Sporadic	Homo	Unaffected	Effective

Table 2 | The different RBM20 mutations identified in DCM patients. Residues within the RSRSP stretch in the RS-rich region are colored in red [26].

3. *RBM20 controls heart-specific alternative splicing*

In a recent study, genome-wide analysis of cardiac transcriptome from *RBM20*-deficient rats and human DCM patients with *RBM20* missense mutations revealed a set of 31 genes that are alternatively spliced by RBM20, many of which are associated with cardiomyopathies and cardiac cell biology [26, 28]. Specifically, RBM20 protein was shown to bind to the UCUU element in the nascent transcripts in human cells as well as in rat cardiomyocytes. This element serves as a precise RNA recognition element (RRE) for RBM20 that is conserved across species [26, 33]. The UCUU motif is predominantly enriched within introns, such that binding of the RBM20 protein to intronic regions near 3' and 5' splice sites of target exons, and in close proximity to the U1 and U2 snRNPs' binding sites, leads to the repression of these exons' splicing [33]. Transcripts of 18 genes having the UCUU motif, including several cardiac-expressed genes, were shown to directly bind RBM20. Interestingly, one of these genes is the *TTN* gene, which encodes the titin protein, and plays an essential role in the DCM phenotype [33]. In addition to *TTN*, transcripts of 17 other genes were shown to be directly regulated by RBM20, most commonly by mutually exclusive splicing. These are: *CamkIIδ, DST, ENAH, IMMT, LDB3, LMO7, MLIP, LRRFIP1, MYH7, MYOM1, NEXN, OBSCN, PDLIM3, RTN4, RyR2, SORBS1,* and *TNNT2* [33]. Splicing regulation of mutually exclusive exons is usually correlated with the expression of tissue-specific splice variants. This mechanism here is in accord with the tissue-specific expression pattern of RBM20, which is expressed mainly in the heart [16].

4. *Alternative splicing of TTN gene:*

RBM20 protein regulates the alternative splicing of several sarcomeric proteins, thus affecting sarcomere structure and function. Among these is the *TTN* gene, which encodes the enormously large elastic protein, titin. Titin is responsible for maintaining the structural integrity of the sarcomere and restoring it to normal length after extension and contraction [16].

While almost all exons encoding the Z-band, A-band, and M-band are constitutively included in the mature mRNA of titin, many exons encoding the I-band, which is the elastic region, are the ones that undergo alternative splicing [26].

Mutually exclusive alternative splicing of TTN results in many protein isoforms of roughly 3.0 to 3.9 MDa, the most common are N2B and N2BA [34] (Figure 5). N2B isoform is short and stiff, while N2BA isoforms are long and more compliant. These isoforms can be co-expressed in the same sarcomere, where the ratio of short to long titin isoforms determines myocardial passive stiffness [35].

Differential expression of titin isoforms occurs in a tissue-specific and developmentally regulated manner. N2BA isoforms are predominantly expressed during fetal life, whereas N2B isoform is expressed mainly after birth. This shift in titin isoforms expression is essential for the proper ventricular diastolic function of the developing heart as it allows adjustment of diastolic filling properties: N2B-enhanced passive stiffness of the postnatal heart prevents ventricular overfilling during diastole. [35] [16, 36].

In addition, this switch in titin isoforms after birth is essential for systolic function since N2B isoform has increased Ca2+ sensibility, which leads to improved contractility during systole [16, 37].

Studies have shown that in rats harboring a heterozygous *RBM20* mutation, titin N2B isoform was no longer expressed whereas the long N2BA isoform was predominantly expressed. Also, homozygous *RBM20* mutant rats exclusively expressed the extremely long N2BA-G titin isoform [26, 28] (Figure 5B). This shift in isoforms' expression was also found in the hearts of DCM patients carrying a heterozygous missense mutation S635A in *RBM20* gene, where the N2BA titin isoform was found to be predominantly expressed [26, 28]. Besides, in a human heart-failure cohort, differential expression levels (high vs. low) of endogenous RBM20 significantly affected the splicing pattern of *TTN* [33]. These findings indicated that the splicing of many of the *TTN* gene exons is very sensitive to the amount of functional RBM20 protein [26]. Moreover, the expression of the long N2BA titin isoform when *RBM20* is mutated or downregulated explains the dilated heart phenotype in the affected patients.

In the *TTN* pre-mRNA, RBM20-binding sites were found in many introns between exon 50 and exon 219, suggesting that RBM20 alternatively splices titin through binding to these sites and repressing exons 51-218 by inhibiting the excision of most if not all of the introns in this region [26].

A)

B)
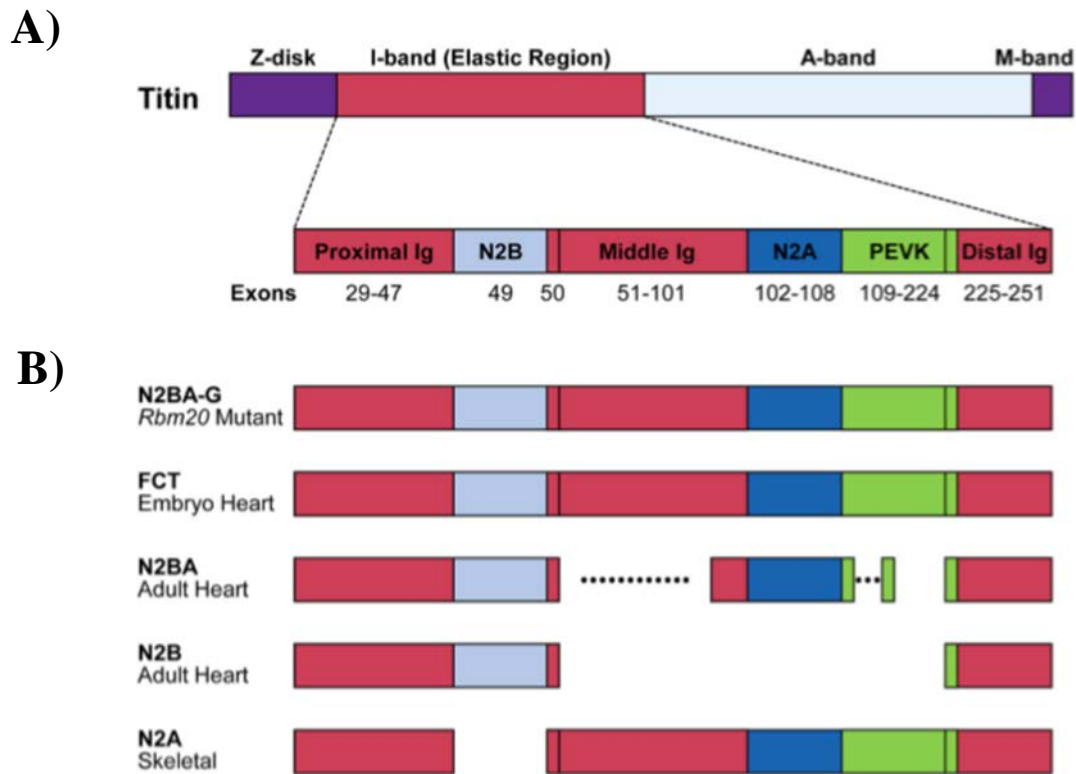
Figure 5 | Structure of the different titin protein isoforms. **(A):** Schematic showing the domains of the titin protein, their names, position, as well as their corresponding exons. **(B):** Schematic of the structure of titin isoforms, their names, and the tissues that mainly express them. Dotted lines indicate highly variable alternatively spliced regions. Abbreviations: **FCT**: fetal cardiac titin [26].

5. *Alternative splicing of other genes:*

In addition to *TTN*, RBM20 regulates the alternative splicing of Ca2+- and ion-handling genes, most notably *CAMK2D* and *RYR2* [25].

CAMK2D gene encodes the Ca2+/calmodulin-dependent protein kinase II-δ (CamkIIδ), which phosphorylates proteins of the sarcomere, calcium channels, and transcription factors. Deregulations of CamkIIδ thus affect cell signaling, Ca2+ handling, and gene expression. Interestingly, DCM-associated *RBM20* mutation leads to an isoform switch from CamkIIδB to CamkIIδA. These two isoforms are both expressed

in the healthy heart [38]; however, CamkIIδB is mainly located in the nucleus where it regulates gene expression, whereas CamkIIδA is predominantly found in T-tubules where it plays a role in the facilitation of the L-type calcium channel (LTCC) [16, 39]. This isoform switch leads to an increased L-type calcium current, intracellular Ca2+ overload, and increased sarcoplasmic reticulum Ca2+ in the RBM20-depleted myocytes. These changes ultimately lead to excitation-contraction coupling defects, and increase the risk of tachyarrhythmia in affected patients [16, 40].

RBM20 loss or mutation also leads to aberrant splicing of the *RYR2* gene, which encodes the ryanodine receptor protein 2 (RyR2). *RYR2* is mainly expressed in the heart and is one of the key components of the major calcium release channel for excitation-contraction coupling in the sarcoplasmic reticulum membrane [33]. Missplicing of this gene leads to the inclusion of a 24-bp exon in the mature RyR2 protein, leading to its translocation from the endoplasmic reticulum (ER) to the intranuclear cisternae. This mislocalization deeply affects calcium signaling and causes arrhythmias and sudden death, which are both complications of *RBM20*-related DCM [16, 33, 41].

6. *RBM20 interacting partners*

To date, much work has been done to uncover the process in which *RBM20* mutation or downregulation leads to the Dilated Cardiomyopathy phenotype. However, not much is known about the molecular mechanism of RBM20-related DCM and the biological function of this protein. Thus, it is important to shed more light on the network of protein interacting partners of RBM20. Therefore, Dr. Jaalouk's lab team

used phage display biopanning technique in order to find potential interacting partners of RBM20.

a. <u>Description of Phage Display Assay</u>

Phage display is a powerful in vitro screening technique that allows researchers to identify peptides with high affinity and specificity for the target of interest. It is used for studying protein-ligand interactions, most frequently applied for protein-protein, protein-peptide, and protein-nucleic acids interactions. In this technique, the genetic code for a protein/peptide is inserted in the genome of a filamentous phage (most frequently M13 bacteriophage) that subsequently displays this protein on its surface as a fusion to natural coat protein. This way, libraries of up to 10^{10} protein/peptide variants can be constructed, where each phage expresses a random sequence. These libraries are then tested against ligand(s) of interest. Proteins/peptides binding to the specific target of interest are isolated by 3-5 rounds of affinity-driven biopanning and subsequently identified by sequencing the genome of the phages displaying them [42, 43].
The key advantage of phage display is that it saves time while still giving highly specific results. It allows researchers to identify target-binding proteins from a library of millions of different proteins without the need to test and screen each protein individually.

b. <u>Application of Phage Display on RBM20</u>

Using phage display biopanning, Dr. Jaalouk's lab team isolated novel peptides (phage inserts) that selectively bind to the C-terminal fragment of recombinant human RBM20 protein following successive rounds of panning using a random M13 filamentous phage library (Ph.D.- C7C library, NE Biolabs). Two screens of phage

display bio-panning were successfully performed. In the first screen, phage display bio-panning was performed without acid elution in order to identify weak binding partners. After exposing the bacteriophage library to the C-terminal fragment of recombinant human RBM20 protein, and washing out the unbound phages, the bound phages were directly rescued by E-coli infection (Figure 6). Following four successive rounds of biopanning, significant enrichment in phage binding was obtained in Rounds III and IV, where a 2.1 and 2.9 fold change in relative phage binding units was detected, respectively (Figure 7A). In the second screen, phage display bio-panning was performed with acid elution in order to identify strong binding partners. Post binding, bound phages were rescued by acid elution followed by neutralization, and then E-coli infection (Figure 6). After four successive rounds of biopanning, significant enrichment of phage binding was obtained in round IV, where a 2-fold increase in relative phage binding units was detected (Figure 7B). Bound phages from each round were isolated, and the DNA inserts in phage plaques were sequenced using PCR to identify the displayed peptides. Next, enriched peptides from the first and second screens were determined, and proteins that are mimicked by these peptides were identified and considered as putative RBM20-interacting proteins. Among these identified putative interacting partners with RBM20 is NOTCH2 protein, which is the protein of interest in this thesis (Table 3 & 4).
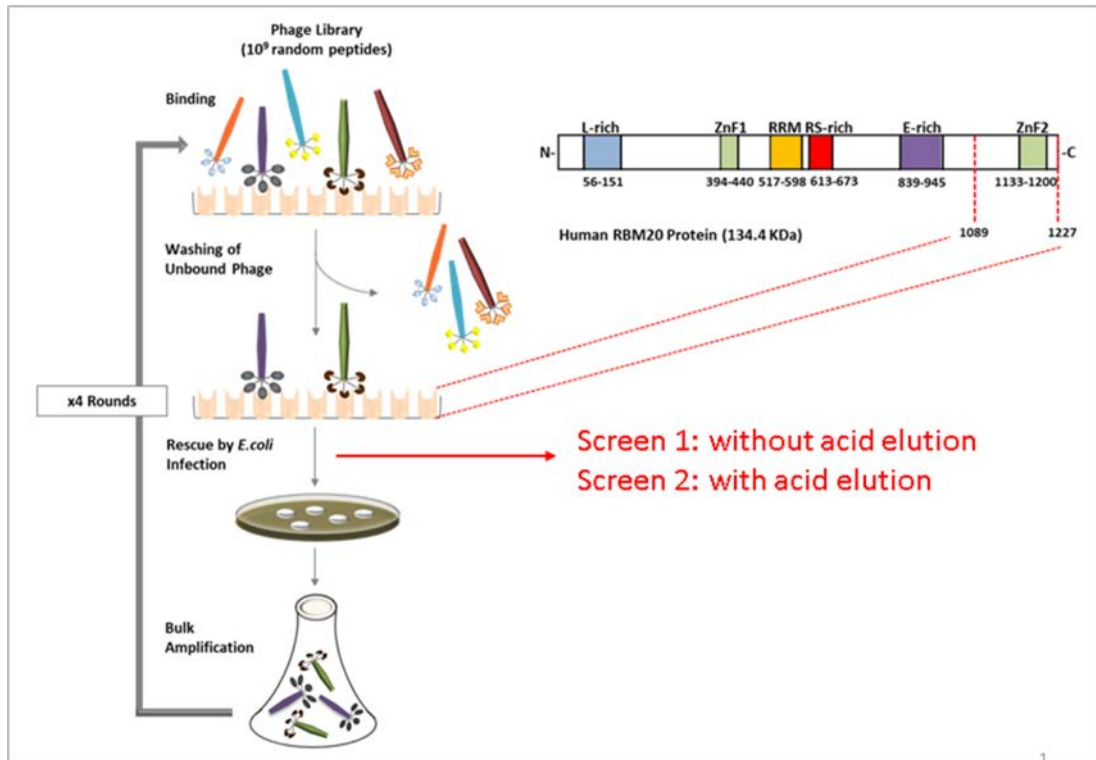
Figure 6 | Schematic showing the phage display screening using the C-terminal fragment of recombinant human RBM20 protein (C-RBM20). (Figure by Dr. Hind Zahr)
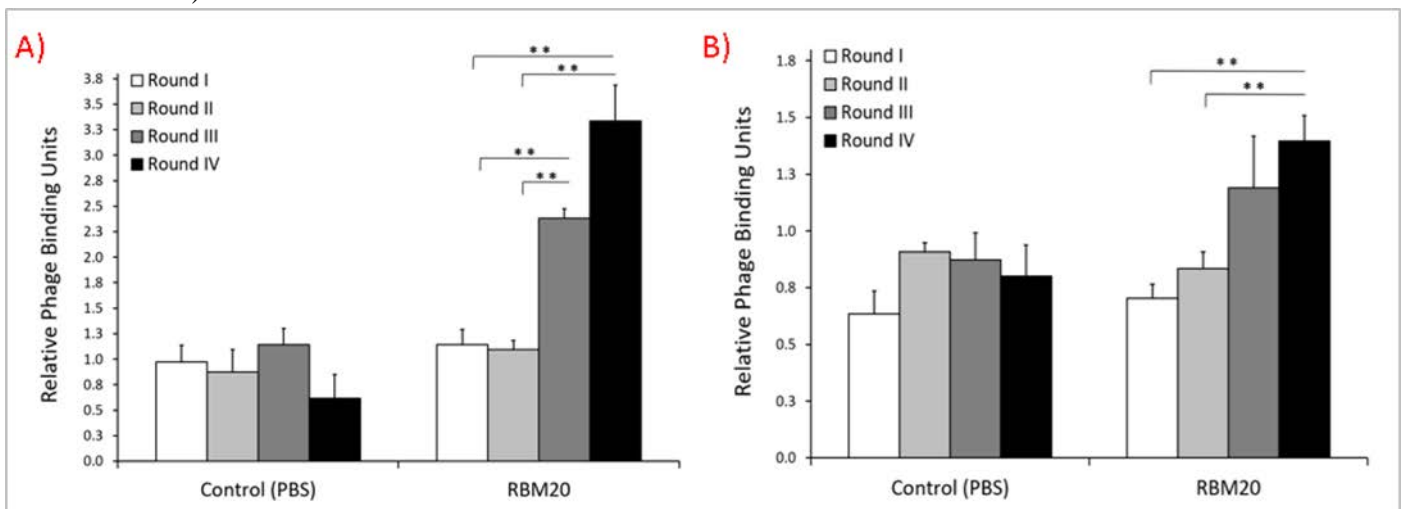
Figure 7 | Phage display biopanning scheme. **Panel A:** Phage display biopanning without acid elution resulted in significant enrichment in phage binding in rounds III (2.1-fold increase) and IV (2.9-fold increase). **Panel B:** Biopanning with acid elution resulted in significant enrichment in phage binding in round IV (2-fold increase).

Screen/ Round	Peptide (% Frequency)	Matching motif	Protein Mimic (gene)
S1/RI	TVNEGMT (98)	651-**INEGMT**-656	Piwi-like protein 1: PIWIL1 (Piwil1)
		36-**VNEGM**-40	Neurogenic locus notch homolog protein 2: NOTCH2 (Notch2)
		228-**VNEGM**-232	Probable cation-transporting ATPase 13A5: ATP13A5 (Atp13a5)
		490-**TVTDGMT**-496	Protein sidekick-1: SDK1 (Sdk1)
		647-**VTEGMT**-652	Cullin-9: CUL9 (Cul9)
		1190-**VNAGMT**-1195	Dedicator of cytokinesis protein 9: DOCK9 (Dock9)
S1/RII	MVRDHSV (94)	6834-**MVRDH**-6838	Nesprin-1: SYNE-1 (Syne-1)
		346-**MIRDHEV**-352	Rho GTPase-activating protein 25: ARHGAP25 (Arhgap25)
		1650-**MVVDHSV**-1656	Protein furry homolog: FRY (Fry)
		173-**VREHSV**-178	Kinesin-like protein: KIF13B (Kif13b)
		472-**MVRQHS**-477	Zinc finger protein ZXDC: ZXDC (Zxdc)
		622-**VREHSV**-627	Protein FAM83G: FAM83G (Fam83g)
S1/RIII	MVRDHSV (88)	6834-**MVRDH**-6838	Nesprin-1: SYNE-1 (Syne-1)
		346-**MIRDHEV**-352	Rho GTPase-activating protein 25: ARHGAP25 (Arhgap25)
		1650-**MVVDHSV**-1656	Protein furry homolog: FRY (Fry)
		173-**VREHSV**-178	Kinesin-like protein: KIF13B (Kif13b)
		472-**MVRQHS**-477	Zinc finger protein ZXDC: ZXDC (Zxdc)
		622-**VREHSV**-627	Protein FAM83G: FAM83G (Fam83g)
S1/RIV	MVRDHSV (100)	6834-**MVRDH**-6838	Nesprin-1: SYNE-1 (Syne-1)
		346-**MIRDHEV**-352	Rho GTPase-activating protein 25: ARHGAP25 (Arhgap25)
		1650-**MVVDHSV**-1656	Protein furry homolog: FRY (Fry)
		173-**VREHSV**-178	Kinesin-like protein: KIF13B (Kif13b)
		472-**MVRQHS**-477	Zinc finger protein ZXDC: ZXDC (Zxdc)
		622-**VREHSV**-627	Protein FAM83G: FAM83G (Fam83g)

Table 3 | High frequency peptides from phage display biopanning on the C-terminal fragment of recombinant human RBM20 protein without acid elution (Screen 1)

Screen/ Round	Peptide (% Frequency)	Matching motif	Protein Mimic (gene)
S2/RI	TVNEGMT (86)	651-**INEGMT**-656	Piwi-like protein 1: PIWIL1 (Piwil1)
		36-**VNEGM**-40	Neurogenic locus notch homolog protein 2: NOTCH2 (Notch2)
		228-**VNEGM**-232	Probable cation-transporting ATPase 13A5: ATP13A5 (Atp13a5)
		490-**TVTDGMT**-496	Protein sidekick-1: SDK1 (Sdk1)
		647-**VTEGMT**-652	Cullin-9: CUL9 (Cul9)
		1190-**VNAGMT**-1195	Dedicator of cytokinesis protein 9: DOCK9 (Dock9)
S2/RII	TVNEGMT (72)	651-**INEGMT**-656	Piwi-like protein 1: PIWIL1 (Piwil1)
		36-**VNEGM**-40	Neurogenic locus notch homolog protein 2: NOTCH2 (Notch2)
		228-**VNEGM**-232	Probable cation-transporting ATPase 13A5: ATP13A5 (Atp13a5)
		490-**TVTDGMT**-496	Protein sidekick-1: SDK1 (Sdk1)
		647-**VTEGMT**-652	Cullin-9: CUL9 (Cul9)
		1190-**VNAGMT**-1195	Dedicator of cytokinesis protein 9: DOCK9 (Dock9)
S2/RIII	MVKDHMA (27)	47-**LVKNHMA**-53	Spermatogenesis-associated protein 7: SPATA7 (Spata7)
		263-**MVIEHMA**-269	Thioredoxin reductase 1: TXNRD1 (Txnrd1)
		167-**MVIEHMA**-173	Selenoprotein K: SELENOK (Selenok)
		459-**MVKDEM**-464	Protein Argonaute-2: AGO2 (Ago2)
		329-**MLEDHMA**-335	TBCC domain-containing protein 1: TBCCD1 (Tbccd1)
		1-**MVKNQM**-6	RNA-binding protein 28: RBM28 (Rbm28)
		6846-**MVRDHL**-6851	Nesprin-1: SYNE-1 (Syne-1)
		6837-**MVRDHL**-6842	Nesprin-1: SYNE-1 (Syne-1)
S2/RIV	TVNEGMT (88)	651-**INEGMT**-656	Piwi-like protein 1: PIWIL1 (Piwil1)
		36-**VNEGM**-40	Neurogenic locus notch homolog protein 2: NOTCH2 (Notch2)
		228-**VNEGM**-232	Probable cation-transporting ATPase 13A5: ATP13A5 (Atp13a5)
		490-**TVTDGMT**-496	Protein sidekick-1: SDK1 (Sdk1)
		647-**VTEGMT**-652	Cullin-9: CUL9 (Cul9)
		1190-**VNAGMT**-1195	Dedicator of cytokinesis protein 9: DOCK9 (Dock9)

Table 4 | High frequency peptides from phage display biopanning on the C-terminal fragment of recombinant human RBM20 protein with acid elution (Screen 2)

D. Notch2 protein

1. Notch family and structure

Notch2 belongs to a family of proteins that comprise the Notch signaling network, an evolutionary ancient, highly conserved intercellular signaling pathway that was first described by Morgan approximately 100 years ago [44]. Notch signaling pathway plays an important role in deciding cellular fate, cellular development, differentiation, proliferation, apoptosis and others. In mammals, the Notch pathway consists of four homologous Notch protein isoforms (Notch 1-4) and five ligands, which are Jagged 1, Jagged 2, Delta-like 1, Delta-like 3, and Delta-like 4 [45].

Notch protein is a single-chain transmembrane protein that has a molecular weight of 300 kDa. Notch extracellular domain (NECD) is composed of 36 epidermal growth factor-like repeats (EGFR) that are responsible for ligand binding, and a negative regulatory region (NRR) which consists of three cysteine-rich LIN12/Notch repeats, and prevents ligand-independent activation by preventing the access of metalloproteinases to the S2 cleavage site of Notch in the absence of ligand [45, 46]. The Notch intracellular domain (NICD) consists of a RAM domain (RAM: RBP-Jk associated molecular domain, where RBP-Jk is recombination signal binding protein for immunoglobulin Jk region), six ankyrin/cdc10 repeats (ANK) flanked by two nuclear localization signals (NLS), a C-terminal Proline-Glutamic acid-Serine-Threonine (PEST) domain, and a transcriptional activation domain (TAD). The RAM and ANK domains interact with the DNA-binding protein RBP-Jk, the TAD region contains phosphorylation sites that are essential for allowing other intracellular domains to modulate Notch signaling, and PEST region is essential for promoting protein instability and degradation of active NICD (Figure 8) [45-47].
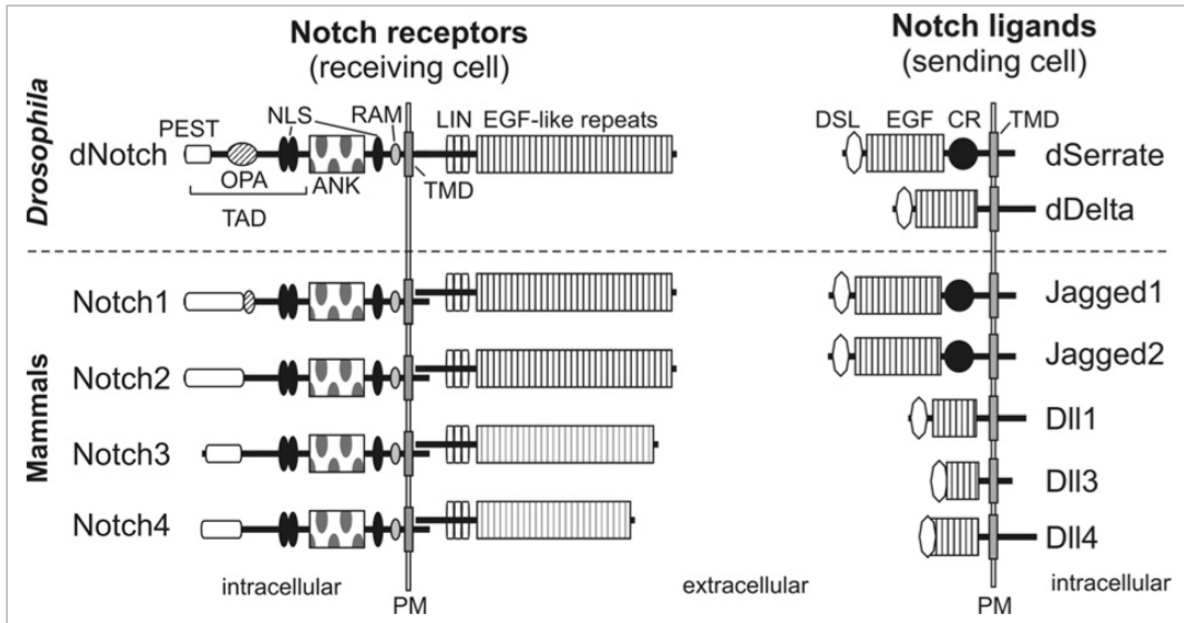
Figure 8 | Schematic showing Notch isoforms, their structure, and their corresponding ligands in Mammals and Drosophila. Abbreviations: **PM**, plasma membrane; **TMD**, transmembrane domain; **PEST**, proline, glutamate, serine, threonine-rich degradation motif; **OPA**, opa repeats; **TAD**, transactivation domain; **NLS**, nuclear localization signals; **ANK**, ankyrinrepeats; **RAM**, RAM domain; **LIN**, LIN12/Notch repeats; **DSL**, Delta-Serrate-Lag2 domain; **EGF**, EGF-like repeats; **CR**, cysteine rich region; **Dll1**, Delta-like ligand 1; **Dll3**, Delta-like ligand 3; **Dll4**, Delta-like ligand 4 [47].

2. Notch signaling cascade

Notch signaling is activated upon binding of the ligand of one cell (Delta or Jagged) to the Notch receptor of an adjacent cell. On the molecular level, this binding promotes two proteolytic cleavage events in the Notch receptor (Figure 9). The first cleavage (S2 cleavage), catalyzed by the ADAM-family of metalloproteases, leads to the release of the extracellular domain of the Notch receptor. S2 cleavage triggers a second cleavage (S3 cleavage), which is mediated by γ-secretase, an enzyme complex that consists of presenilin, nicastrin, PEN2, and APH1. S3 cleavage releases the Notch intracellular domain (NICD) from the cell membrane, which then translocates to the nucleus, directed by its two nuclear localization signals [45, 48]. In the nucleus, NICD

25

acts as a transcription factor coactivator by heterodimerizing with the transcription factor CSL (C̲ promoter-binding factor in humans, S̲uppressor of hairless in Drosophila, L̲AG in Caenorhabditis elegans; also called RBP-Jk in mice) and interacting with the Mastermind co-activator (Mastermind-like transcriptional co- activator 1 (MAML1) in human) [45, 49]. This ultimately leads to the activation of the transcription of target genes. [48]
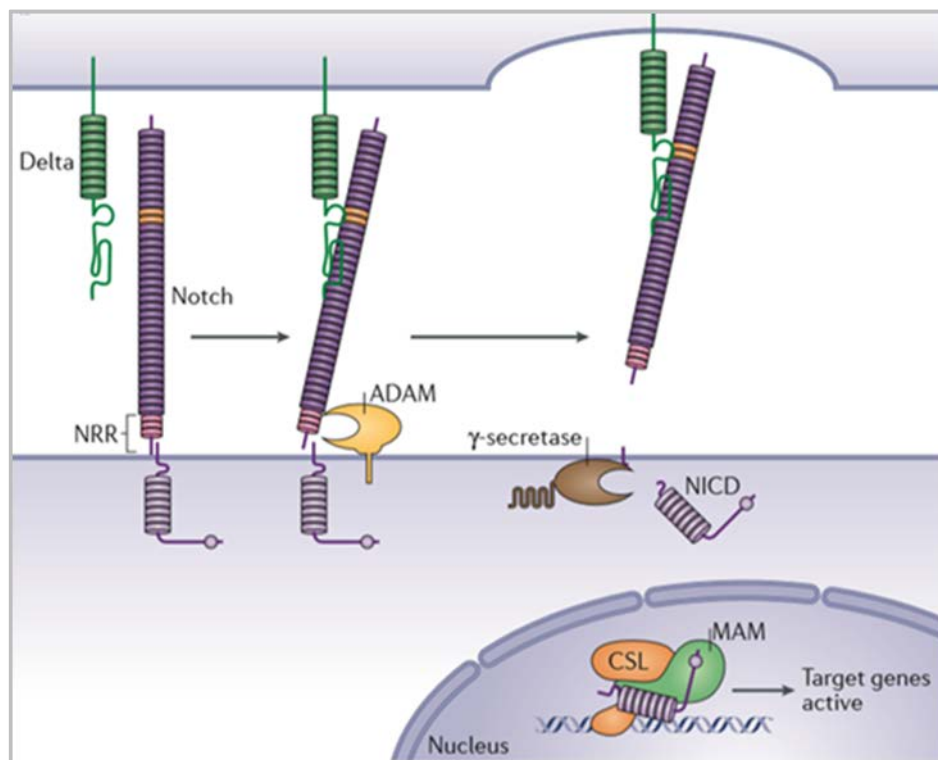
Figure 9 | Schematic summarizing the Notch signaling pathway which begins by binding of the ligand (green) of a cell to the Notch receptor extracellular domain (purple) of an adjacent cell. This elicits two proteolytic events, the first one being by ADAM and the second one by γ-secretase enzyme complex, leading to the release of the Notch intracellular domain (NICD) in the cytoplasm. NICD then translocates to the nucleus and interacts with CSL transcription factor (orange) and MAM co-activator (green), stimulating ultimately the transcription of target genes. Abbreviations: **NRR**: negative regulatory region; **NICD**: Notch intracellular domain; **CSL**: C̲ promoter-binding factor in humans, S̲uppressor of hairless in Drosophila, L̲AG in Caenorhabditis elegans; **MAM**: Mastermind co-activator [49].

3. *Role of Notch signaling*

Notch signaling pathway is essential for a broad spectrum of cellular systems, and its deregulation has been linked to a vast number of diseases and developmental disorders. Indeed, Notch signaling provides effective communication between adjacent cells to regulate adhesion, differentiation, proliferation, cell fate decisions, apoptosis, and epithelial-to-mesenchymal transition (EMT) [45, 47]. Moreover, Notch signaling is involved in the development of the liver, heart, skeleton, vasculature, eye, bone, and other organ systems [50]. Given the profound and widespread roles of Notch signaling across a wide range of tissues, mutations or altered signaling output in this pathway leads to many types of developmental defects and diseases, among them is Alagille syndrome, tumors, CADASIL disease which is a neurologic disorder, and retinal dysplasia to name few. The list of diseases caused by mutations in Notch family members is depicted in table 5 [46, 51].

Gene	Diseases associated with mutated gene	References
DLL3	Spondylocostal dysostosis (axial skeleton segmentation disorder)	(Bonafe et al., 2003; Bulman et al., 2000; Turnpenny et al., 2003; Whittock et al., 2004)
JAG1	Alagille syndrome; patients with *JAG1* mutations display variable phenotypes in bile duct paucity, cardiac defects (including tetralogy of Fallot), posterior embryotoxon, spine defects (including butterfly vertebrae) and deafness	(Bauer et al., 2010; Colliton et al., 2001; Crosnier et al., 1999; Crosnier et al., 2001; Eldadah et al., 2001; Heritage et al., 2002; Heritage et al., 2000; Krantz et al., 1998; Krantz et al., 1999; Li et al., 1997; Oda et al., 2000; Oda et al., 1997; Raas-Rothschild et al., 2002; Ropke et al., 2003; Stankiewicz et al., 2001; Warthen et al., 2006)
LFNG	Spondylocostal dysostosis (axial skeleton segmentation and growth disorder)	(Sparrow et al., 2006)
MAML2	Mucoepidermoid carcinoma, secondary acute myeloid leukemia	(Conkright et al., 2003; Enlund et al., 2004; Tonon et al., 2003)
NOTCH1	T-ALL (T-cell acute lymphoblastic leukemia) Aortic valve disease	(Weng et al., 2004) (Garg, 2006)
NOTCH2	Alagille syndrome Hajdu-Cheney syndrome (progressive and severe bone resorption leading to osteoporosis)	(McDaniell et al., 2006) (Simpson et al., 2011)
NOTCH3	CADASIL (cerebral autosomal dominant arteriopathy with subcortical infarcts and leukoencephalopathy, a hereditary stroke disorder)	(Joutel et al., 1997a; Joutel et al., 2004; Joutel et al., 1997b; Oberstein et al., 1999)
NOTCH4	Debated involvement in schizophrenia	(Ivo et al., 2006; McGinnis et al., 2001; Sklar et al., 2001; Skol et al., 2003; Tochigi et al., 2004; Wang, Z. et al., 2006; Wei and Hemmings, 2000)

Table 5 | Mutations in Notch signaling components and the different human diseases associated with them [51].

4. *Notch2 protein and heart diseases*

Notch signaling is involved in the normal development of the heart during mammalian cardiogenesis, where it promotes the development of the atrioventricular canal, the ventricles, the aortic valve, as well as the outflow tract. In addition, Notch signaling was shown to play an important role in heart regeneration and cardiac repair after injury [45, 50]. Given the importance of Notch signaling in the development of the heart, abnormal Notch signaling can induce a series of heart malformations [45]. The most common diseases include Bicuspid aortic valve, which is caused by abnormal EMT due to *Notch1* mutations, and Aortic valve calcification due to mutations in *Notch1*, *Hey1*, and *Hey2* genes [45]. Mutations in the *Notch2* gene have also been associated with a number of heart malformations and conditions that display cardiac manifestations. Among them are pulmonary artery stenosis, over-riding aorta, hypoplastic right ventricle, ventricular septal defect resembling tetralogy of Fallot, and Alagille syndrome. Indeed, Alagille syndrome is an autosomal dominant disorder characterized by liver, skeletal, eye, and heart defects. Patients of this syndrome have a range of congenital heart defects, including pulmonary artery stenosis, tetralogy of Fallot, and ventricular septal defects [45, 52, 53].

In a recent study, mutations in *Jag1* and *Jag2* genes were found to be associated with deregulations in genes related to dilated, hypertrophic, and arrhythmogenic right ventricular Cardiomyopathy (DCM, HCM, and ARVC). Moreover, *Jag1* inactivation in embryonic myocardium led to the generation of mice with a dilated heart, a thin and

compact myocardium, systolic dysfunction, cardiomyopathy, and reduced ejection fraction [54]. In another study, Jag1 mutations showed structural and functional signs of dilated cardiomyopathy disease [55]. To sum up, mutations in *Jag1* and *Jag2* genes, which are ligands interacting with Notch2 protein, were shown to be associated with dilated cardiomyopathy disease [56].

Interestingly, mutations in *PSEN1* and *PSEN2* genes were also reported to be associated with dilated cardiomyopathy disease. These genes encode the presenilin protein, which takes part in the γ-secretase enzyme complex that is responsible for the S3 cleavage of Notch protein, an important step of the Notch signaling pathway [53].

Taking all together, these findings support our phage display biopanning results and strengthen our hypothesis of a possible interaction between RBM20 and Nocth2 protein, and its implication in the development of the Dilated Cardiomyopathy disease.

E. Gap in knowledge, Study rationale, and Hypothesis

Since *RBM20* identification in 2009 as a gene associated with Dilated Cardiomyopathy disease, much work has been done to uncover the different mutations of this gene, their prevalence among DCM patients, the structure of RBM20 protein, its role, the genes affected by its deregulation, and much more. Despite much progress, the molecular mechanisms underlying *RBM20*-related cardiomyopathies remain to be deciphered, in particular, what is the network of proteins that interact with RBM20 protein, how do they interact and where specifically inside the cell?

To answer these questions, a pilot study was done in Dr. Jaalouk's laboratory to investigate the network of RBM20-interacting partners using phage display biopanning on the C-terminal fragment of recombinant RBM20 protein. As a result, a panel of

putative interacting partners with RBM20 were identified, including Neurogenic Locus Notch Homolog Protein 2 (Notch2 protein), which we chose to be our focus in this current study.

We decided to study the potential interaction between RBM20 and Notch2 protein in particular for many reasons. First, Notch2 protein appeared four times on our phage display screens: one time without acid elution, and three times with acid elution indicating the presence of strong binding between these two proteins. Second, just like all Notch receptors, the Notch intracellular domain (NICD) of Notch2 protein has the ability to migrate to the nucleus where it does its work. Similarly, after being phosphorylated, RBM20 protein translocates to the nucleus where it regulates alternative splicing of target pre-mRNAs. This common localization suggests a potential interaction inside and/or outside the nucleus. Finally, studies have shown that Notch signaling pathway is crucial to the heart organogenesis, and mutations in Notch proteins, and specifically Notch2 protein, have been linked to a spectrum of diseases that display cardiac manifestations, such as Alagille syndrome and Tetralogy of Fallot.

Taken together, in this study, we attempt to investigate the interplay between RBM20 and Notch2 proteins in the development of cardiomyopathies. Our hypothesis suggests that Notch2 interacts with RBM20 in healthy hearts and that cardiomyopathies that arise due to mutations in *RBM20* gene are partly mediated by a disruption in the interaction between RBM20 and Notch2 proteins.

F. Objective of the study and specific aims

Our long term objective is to gain a better understanding of the mechanisms in which *RBM20* mutations lead to the development of the Dilated Cardiomyopathy

(DCM) disease. To this end, delineating the mode of action and identifying the protein interacting partners of RBM20 protein may provide better insight into the pathobiology of *RBM20*-mediated DCM. Accordingly, for the purpose of this study, our specific aims are:

Specific Aim 1:

To assess the expression and the intracellular distribution of Notch2 protein, and to determine if it co-localizes with RBM20 protein using Immunofluorescence staining, upright fluorescent microscope, and confocal microscopy.

Specific Aim 2:

To determine if there is direct interaction between RBM20 and Nocth2 proteins, using Co-Immunoprecipitation and Proximity Ligation assays (PLA).

G. Significance of the study

The validation of Notch2 as an interacting partner with RBM20 would provide a better mechanistic insight into the RBM20 bio-function, or lack thereof, and in its role in influencing the cardiomyopathy phenotype, hence offering new clues into the molecular mechanisms responsible for the pathogenesis of this devastating complex disease. In addition, identification of such an interaction may lead to the development of better diagnostic and therapeutic modalities for cardiomyopathies, which would ultimately significantly impact the quality of life for the patients.

CHAPTER II

MATERIALS AND METHODS

A. Cell lines

RD cells are cancerous human skeletal muscle cells that are derived from a 7-years old girl with Rhabdomyosarcoma disease. These cells were purchased from American Type Culture Collection (ATCC).

Despite being a skeletal muscle lineage, we chose to use the RD cell line in our study, and this is for many reasons. First, we preferred to start with it over H9c2 cells, which are rat heart myoblasts because RD cells can be propagated more owed to it being an immortalized cell line. It is important to note here that we will use H9c2 cells and rat left ventricular cells in future studies to confirm the results found in this study on RD cells. Second, RD cells were found to express the highest amount of RBM20 and Notch2 proteins compared to C2C12 cells (immortalized mouse skeletal myoblast cell line) and MEFs cells (Immortalized Mouse Embyo Fibroblast) (Figure 10). Thus, this cell line will ultimately give us the most evident results.
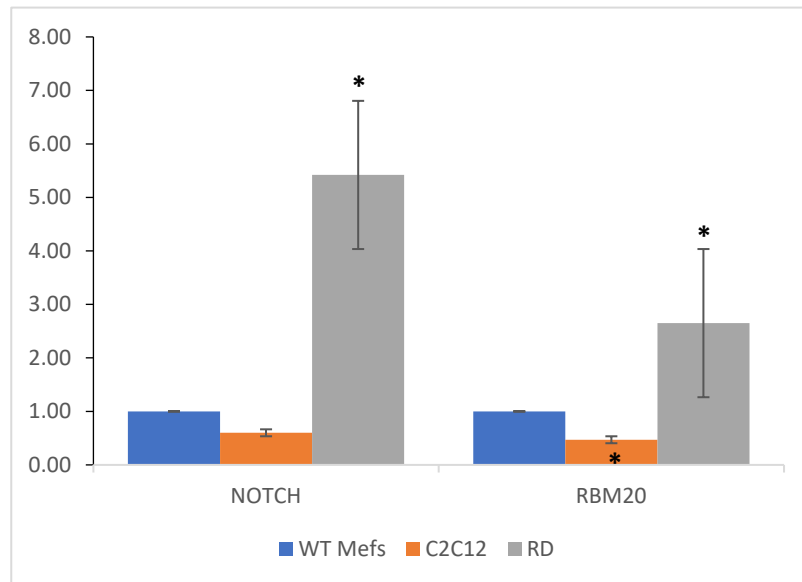
Figure 10 | Western Blot analysis of Notch2 and RBM20 expression in C2C12, MEFs, and RD cell lines normalized to the loading control Lamin A/C. Image J analyses showed an increase in Notch2 and RBM20 expression normalized to that of Lamin A/C in RD cells in comparison to C2C12 and MEFs. Results were checked for statistical significance by one-way ANOVA test.

1. *Cell culture*

Adherent RD cells were propagated in tissue culture using specialized media consisting of Dulbecco's Modified Eagle's Medium DMEM media (Cat.# D6429, Sigma-Aldrich), supplemented with 10% Fetal Bovine Serum (FBS) (Cat.# 9665, Sigma-Aldrich), and 1% penicillin-streptomycin (Cat.# DE17-602E, Lonza). Cells were cultured at 37°C in a humidified incubator at 5% CO_2. When monolayer cells in the T-75 flask reached 80-85% confluency, they were rinsed once with 3 ml of 1X Dulbecco's Phosphate Buffered Saline without Ca^{2+} and Mg^{2+} (PBS) (Cat.# RNBG7730, Sigma). Next, 2 ml of 1X Trypsin-EDTA (Sigma) were used to detach the cells from the surface of the 75cc-flask. Cells were then incubated at 37°C and 5% CO_2 for 30 sec-1 min, resuspended in 7 ml of complete growth medium to inactivate the trypsin, and centrifuged at 160xg at 4°C for 7 min. Cell pellet was resuspended with complete

growth medium, and an appropriate volume of cells was pipetted into new cell culture
flasks pre-filled with complete growth medium. Cells were splitted and passaged twice
per week.

2. *Cell count*

In order to accurately determine the number of viable cells from the total
population of cells in the T-75 flask, cell counting was performed using Trypan blue
vital exclusion stain (Cat.# 17-942E, Lonza) and a hematocytometer. After
resuspending the cell pellet in 1 ml of complete media, 10 µl of the cells was removed
and mixed with 10µl of Trypan blue in an Eppendorf for counting. Then, depending on
seeding density, an appropriate volume of cells was taken and mixed with complete
media to be distributed to cell culture flasks.

B. Immunofluorescence staining (IF)

RD cells that are 80% confluent in T-75 flask were seeded at 1:12 in 6-well-
plates on 22 x 22 mm wide square cover glass (OmegaLab) using 3 ml of complete
media per well. Cells were left to adhere for two nights in a humidified incubator at
37°C, 5% CO2 until they reached 75-80% confluence. Then, cells were rinsed twice
with 2 ml of 1x PBS, 5 minutes each. Before proceeding with the experiment, cells were
checked for confluence and spreading using a phase-contrast microscope. Next, multiple
fixation methods and protocols were used.

1. *PFA method (Co-localization)*
a. Co-localization of Rbm20 and Notch2

For the Paraformaldehyde (PFA) fixation method, cells were fixed with 2 ml of 4% PFA in 1X PBS at room temperature for 10-15 minutes without nutating. The 4% PFA was freshly prepared by diluting stock of 40% PFA solution (Paraformaldehyde, Cat.# 28906, Thermo Scientific) using 1X PBS. Cells were washed four times in 2 ml of 1X PBS; a quick first wash followed by three washes, 5 min each. Then, cells were permeabilized using 1.5 ml of freshly prepared 0.2% Triton-X in 1X PBS at room temperature for 10 min. The 0.2% Triton-X solution was prepared by diluting a working stock of 10% Triton-X in 1X PBS. This latter is considered a transitional dilution and is prepared from 50% Triton-X in 1X PBS solution that was also prepared by diluting the original stock of 100% Triton-X (t-Octylphenoxypolyethoxyethanol, Cat.# T8787, Sigma-Aldrich). Following permeabilization, cells were washed three times in 2 ml of 1X PBS; a first quick wash followed by two washes, 5 min each. Next, cells were blocked using 2 ml of 3% BSA in 1X PBS at room temperature for 2 hours. The 3% BSA solution was prepared by diluting the stock of 10% BSA in 1X PBS solution stored at -20°C. This latter was prepared by diluting the BSA powder (Bovine Serum Albumin, Cat.# A3059, Sigma Aldrich) in 1X PBS. After 2 hours of blocking, the blocking media was removed, and cells were washed once with 2 ml of 1X PBS for 5 min. The coverslips were then transferred to a humidified tray using fine tip forceps and flipped onto 200 µl of the primary antibody of interest added over a piece of parafilm. The tray was then covered with aluminum foil and incubated in the fridge at 4°C overnight. All primary antibodies were prepared as recommended according to the manufacturer's specifications and were diluted in 1% BSA in 1X PBS. Cells were incubated with Rbm20 (D-20), a goat polyclonal IgG provided at 200 µg/ml, and used

at 1:100 (sc-243941, Santa Cruz Biotechnology). Following incubation with the primary antibody, coverslips were returned to the 6-well-plate, while ensuring that the cells were properly oriented to the up for washing. Next, cells were washed three times using 2 ml of 1X PBS, 5 minutes each. Afterward, cells were incubated with the second primary antibody by following the same previously mentioned steps and placed in the fridge at 4°C overnight. This second primary antibody should be raised in a specie other than the first primary antibody used. In this study, we used the Notch2 (D76A6) XP, which is a rabbit monoclonal antibody provided at 515 µg/ml and used at 1:100 (5732S, Cell Signaling Technology). Then, coverslips were returned to the 6-well- plate as previously mentioned and washed three times using 2 ml of 1X PBS, 5 min each. Next, cells were incubated with 200µl of a mixture of two Alexa Fluor-conjugated secondary antibodies prepared in PBS only, each specific to one of the used primary antibodies. Incubation was on a tray as previously described for 1 hour at room temperature in the dark. The secondary antibody used for Rbm20 is Alexa Fluor® 488 donkey anti-goat IgG (H&L) provided at 2 mg/ml and used at 1:500 (ab150133, Abcam), whereas for Notch2 we used Alexa Fluor® 647 donkey anti-rabbit IgG (H&L) provided at 1.95-2 mg/ml and used at 1:500 (ab150075, Abcam). Following incubation, cells were washed three times with 2 ml of 1X PBS, 5 min each. Secondary-only incubated coverslips were used as negative controls to demonstrate low non-specific binding of the secondary antibody. Finally, coverslips were mounted on glass slides that were previously labeled and cleaned with Kim wipes and distilled water. This step was carried out by putting one drop of the mounting medium onto the glass slides, in the absence of light, and placing the coverslip with the cells facing down after removing excess 1X PBS

remaining on the coverslip due to the washing steps by holding the coverslip vertically against a Kim wipe. The mounting medium used is the Ultra-Cruz^{TM} Hard-Set mounting Medium provided as a 10 ml solution containing 1.5 µg/ml of 4',6-diamidino-2-phenylindole (DAPI) as a DNA counterstain (sc-359850, Santa Cruz Biotechnology). Next, the excess mounting medium was removed using the tip of a folded Kim wipe, and the edges of the coverslips were sealed with clear nail polish. Then, slides were placed in a slide box in the dark at room temperature overnight for microscopic imaging. The next day, cells were imaged and then placed at 4°C in the dark for long-term storage.

2. Acetone-methanol method

In the acetone-methanol fixation method, cells were fixed with 200 µl of 100% pure pre-cooled methanol that was placed at -20°C. Methanol was added to the wells under the fume hood in order to prevent any inhalation of this chemical, and then the 6-well plate was gently swirled and incubated in the -20°C freezer for 10 minutes. After fixation, excess methanol was removed under the fume hood, and cells were permeabilized with 200 µl of 100% pure pre-cooled acetone that was also placed at -20°C. Then, the 6-well plate was gently swirled, and the cells were incubated for one minute at -20°C. Next, cells were washed three times with 2 ml of 1X PBS, 5 minutes each; one time under the fume hood and twice on bench. Afterward, cells were blocked using 2 ml of 2% BSA in 1X PBS at room temperature for 1 hour. The 2% BSA solution was prepared by diluting the stock of 10% BSA in 1X PBS solution stored at -20°C. This latter was prepared by diluting the BSA powder in 1X PBS. After 1 hour of blocking, the blocking media was removed, and cells were washed once with 2 ml of

1X PBS for 5 min. The following steps in this assay differ based on two variables. First, we used several primary antibodies for both RBM20 and Notch2 proteins. Also, we attempted to co-localize these two proteins, and to localize each of them alone.

a. Co-localization of Rbm20 and Notch2

After blocking with 2% BSA and washing it away, we transferred the coverslips to a humidified tray using fine tip forceps and flipped them onto 200 µl of Rbm20 primary antibody added over a piece of parafilm. The tray was then covered with aluminum foil and incubated in the fridge at 4°C overnight. The used primary antibody is the Rbm20 (D-20), a goat polyclonal IgG provided at 200 µg/ml, and used at 1:100 by diluting it in 1% BSA in 1X PBS (sc-243941, Santa Cruz Biotechnology). Following incubation with the Rbm20 primary antibody, coverslips were returned to the 6-well-plate, while ensuring that the cells were on the upper side of the coverslips for washing. Next, cells were washed three times using 2 ml of 1X PBS, 5 minutes each. Afterward, cells were incubated with 200 µl of the Alexa Fluor-conjugated secondary antibody on a tray prepared as previously mentioned and placed at room temperature in the dark for one hour. We used several secondary antibodies for Rbm20. These are Alexa Fluor® 488 donkey anti-goat IgG (H&L) provided at 2 mg/ml and used at 1:500, diluted in 1X PBS (ab150133, Abcam), and Alexa Fluor® 647 donkey anti-goat IgG (H&L) provided at 2 mg/ml and used at 1:500, diluted in 1X PBS (ab150131, Abcam). After one hour of incubation, coverslips were returned to the wells, and cells were washed three times with 2 ml of 1X PBS, 5 min each. Next, coverslips were transferred again to a prepared tray and incubated with 200 µl of the Notch2 primary antibody at 4°C overnight. In this study, we used two primary antibodies for Notch2, one of them is already conjugated to

Alexa Fluor® 647. The other primary antibody used is not conjugated to a fluorophore

and is the Notch2 (D76A6) XP, a rabbit monoclonal antibody provided at 515 µg/ml

and used at 1:100 by diluting it in 1% BSA (5732S, Cell Signaling Technology).

Following incubation, in the case of the pre-conjugated Notch2 primary antibody,

coverslips were returned to wells, and cells were washed three times with 2 ml of 1X

PBS, 5 min each. Then, coverslips were directly mounted on labeled and cleaned glass

slides by using the same reagents and following the same steps as in the PFA fixation

method. Finally, slides were placed in a slide box overnight in the dark at room

temperature for microscopic imaging, and the next day, cells were imaged and then

placed at 4°C in the dark for long-term storage. In the case of the un-conjugated Notch2

primary antibody, coverslips were placed back in the 6-well plate, and cells were

washed three times with 2 ml of 1X PBS, 5 min each. Then, cells were incubated with

200 µl of the Alexa Fluor-conjugated secondary antibody prepared in 1X PBS only at

room temperature for one hour. The secondary antibodies used for Notch2 are Alexa

Fluor® 488 donkey anti-rabbit IgG (H&L) provided at 2 mg/ml and used at 1:500

(ab150073, Abcam), and Alexa Fluor® 647 donkey anti-rabbit IgG (H&L) provided at

1.95-2 mg/ml and used at 1:500 (ab150075, Abcam). Following incubation with

secondary antibody, cells were washed three times with 2 ml of 1X PBS, 5 minutes

each, and then mounted on glass slides using mounting medium as previously described.

Note that secondary-only incubated coverslips were used as negative controls to

demonstrate low non-specific binding of the secondary antibody.

b. Localization of RBM20 and Notch2 separately

After washing away the blocking solution, coverslips were transferred to a prepared tray as previously described, where 200 µl of the primary antibody of interest was added over a clean piece of parafilm. Cells were incubated with the primary antibody in the 4°C fridge overnight. The primary antibodies used in this study are Notch2 (D76A6) XP, a rabbit monoclonal antibody provided at 515 µg/ml and used at 1:100 by diluting it in 1% BSA (5732S, Cell Signaling Technology), and Rbm20 unconjugated rabbit polyclonal antibody provided at 1 µg/µl and used at 1:100 by diluting it in 1% BSA (bs-9606R, Bioss). Following incubation with either Notch2 or RBM20 primary antibody, coverslips were returned to the wells, and cells were washed three times with 2 ml of 1X PBS, 5 min each. Next, cells were incubated with 200 µl of the Alexa Fluor-conjugated secondary antibody at room temperature for one hour. We used the same secondary antibody for the staining of both RBM20 and Notch2 proteins. The secondary antibody used was Alexa Fluor® 647 donkey anti-rabbit IgG (H&L) provided at 1.95-2 mg/ml and used at 1:500 by diluting it in 1X PBS (ab150075, Abcam). Secondary-only incubated coverslips were used as negative controls to demonstrate low non-specific binding of the secondary antibody. Finally, we washed the cells three times with 2 ml of 1X PBS, 5 minutes each, and then mounted the coverslips on cleaned and pre-labeled glass slides using mounting medium. This step was carried out as previously described, but using two different mounting media. We used the Ultra-CruzTM Hard-Set mounting Medium, which is provided as a 10 ml solution containing 1.5 µg/ml of 4',6-diamidino-2-phenylindole (DAPI) as a DNA counterstain (sc-359850, Santa Cruz Biotechnology), and the ProLongTM Gold antifade reagent with DAPI, which is provided as a 10 ml solution (Cat#. P36941, ThermoFisher

Scientific). Afterward, we stored the slides at room temperature in the dark overnight. The next day, stained cells were imaged then placed at 4°C in the dark for long-term storage.

C. Microscopic Imaging and Analysis of Results

Image acquisition was performed within 24 to 48 hrs. of staining using the Upright Fluorescent Microscope (DFC7000 T, Leica, CRSL facility) or using the LSM710 Confocal Microscope (Zeiss, DTS facility). Stained cells were first examined using a standard phase-contrast microscope to assess their overall confluence, integrity and spreading. Fluorescent image acquisition was done with 20x and 40x objective magnification where we acquired five frames per slide on average. For the confocal microscopy images, we used the 63x oil objective magnification and we acquired 10 frames per slide on average. Acquired images from the confocal microscope were analyzed by subjective assessment of the subcellular localization of RBM20 and Notch2 proteins inside of RD cells according to the localization of the cell nucleus colored in blue (DAPI). RD cells present in each frame were first counted, then the distribution of the proteins of interest in each cell was assessed and categorized into: Nucleus only, Cytoplasm only, Nucleus > Cytoplasm, or Cytoplasm > Nucleus. Data were next plotted in a bar graph using GraphPad Prism 8 software.

D. Protein extraction, SDS-PAGE, and Western Blotting

1. Protein extraction

Protein extraction from RD cells was done on bench where all steps were performed on ice. RD cells were seeded in T-75 flasks in complete media. When the

cells reached 85-90% confluency, we washed them twice with 5 ml of pre-cooled 1X

PBS without Ca2+ and Mg2+. Next, we added 350 µl of lysis buffer supplemented with

Protease and Phosphatase inhibitors. The lysis buffer was freshly prepared by mixing

343 µl of RIPA buffer (Cat. # SLBS6830, Sigma) with 3.5 µl of Protease inhibitor

cocktail III (Cat. # 22020008-1, bioWORLD) and 3.5 µl of Phosphatase inhibitor

cocktail II (Cat. # L41600092-1, bioWORLD). Cells were then incubated with the lysis

buffer in the cold room at 4°C on a shaker for 30 minutes. Afterward, we collected the

cells using a cell scraper to lodge off lysate clusters from the T-75 flask, and transferred

the cell lysate to a pre-cooled sterile microfuge tube. This latter was then centrifuged at

14,000 rpm at 4°C for 10 min. Following centrifugation, the supernatant containing the

protein extracts was carefully transferred to a labeled pre-cooled fresh microfuge tube

and stored at -20°C.

2. *Sample Protein Quantification*

Protein quantification was performed in 96-well plates. Standardization was

performed using specific dilutions of 1 mg/ml BSA in double distilled water (ddH2O).

200 µl of the Optiblot Bradford Reagent (Cat. # ab119216, Abcam) was added to the

standard and sample wells. Measurement of protein contents was performed on λ= 595

nm.

3. *SDS-PAGE: Sodium Dodecyl Sulfate-Polyacrylamide Gel Electrophoresis*

a. Casting and Gel Preparation

The running (migration) and stacking gels were hand casted with short plates

and spacer plates with a 1.5 mm integrated spacer. First, the short plate and spacer plate

were evenly aligned and slid into the casting frame, which was then placed into the casting stand, the short plate being to the front. To prepare the 6%- acrylamide migration gel, we mixed an appropriate amount of 30% Acrylamide (Cat. # 79-06-1, Sigma Aldrich), ddH2O, Tris-HCl (1.5M, pH= 8.8), 10% SDS (Sodium Dodecyl Sulfate, Cat. # 151-21-3, Sigma Aldrich), 10% APS (Ammonium Persulfate, Cat. # 7721-54-0, Sigma Aldrich) and TEMED (Tetramethylethylenediamine, Cat. # 1610801, Bio-Rad). This mixture was immediately vortexed and smoothly poured to the lower green mark of the casting frame using a glass pipette. Then, we immediately overlaid the top of the migration gel with isobutanol to keep the gel surface flat and to remove the bubbles, if any. The migration gel was left for 30-40 min to polymerize. Then the isobutanol solution was removed. Similarly, a 4% stacking gel was prepared by mixing an appropriate amount of 30% Acrylamide, Tris-HCl (1M, pH= 6.8), 10% SDS, ddH2O, 10% APS and TEMED. The stacking solution was next vortexed and poured on top of the migration gel until the top of the short plate was reached. The comb was immediately seated between the glass plates by aligning the comb ridge with the top of the short plate. The stacking gel was then left for 20-30 min to polymerize and solidify. Meanwhile, the 1x migration buffer was prepared by mixing 800 ml of ddH2O with 200 ml of 5x migration buffer and mixing them on a stirrer at room temperature. A stock of the 5x migration buffer was previously prepared by diluting powdered Tris, Glycine, and SDS in ddH2O to a final concentration of 0.25 M, 1.92 M, and 0.035 M respectively. Casted gels were placed into the electrophoresis chamber with the short plate facing inward. Afterward, the chamber was filled with 1x migration buffer, and the combs were removed vertically and slowly.

43

b. Protein preparation and loading

Samples containing 25 µg of total protein were prepared by mixing the appropriate volume of the protein sample and ddH2O according to the protein quantification results, with 10 µl of 4x Laemmli in sterile pre-cooled microfuge tubes. Samples were then vortexed and denatured at 95°C for 10 min using a heat block. Afterward, samples were stored in the fridge at 4°C to be used the next day, or directly placed on ice to be used immediately. For the protein loading step, we first spinned down the samples for ~1 min using the Ependorf centrifuge. Then, we slowly and vertically loaded 4 µl of the Tricolor Broad Protein Ladder that was stored at -20°C (Cat. # BR0900101, biotechrabbit) in the first well using gel loading tips, and 37 µl of each protein sample in the subsequent wells. In the last well, we loaded 37 µl of 1x Laemmli solution that was freshly prepared by mixing 10 µl of 4x Laemmli with 30 µl of ddH2O. Next, SDS-PAGE was ran at 200 V for approx. one hour or until the blue tracking dye of the Laemmli solution reached the bottom of the gel.

c. Wet Protein Transfer To The Membrane

After the molecular weight-based migration of the proteins through the gel, proteins were transferred from the gel onto a nitrocellulose transfer membrane (Supported Nitrocellulose membrane, Cat. # 1620094, 0.45 µm, Bio-Rad). The nitrocellulose membrane was first cut to the desired size and labeled with the cell line, the experiment number, and the date. Next, two sponges and four blotting papers per gel were also prepared and cut to the same size of the gel. The membrane, sponges and the blotting papers were then soaked in ice-cold 1x transfer buffer that was placed in a large Tupperware. The 1x transfer buffer was prepared by mixing 100 ml of a stock of 10x

transfer buffer with 700 ml of ddH2O, 1 ml of 10x SDS, and 200 ml of 100% Methanol. This mixture was then placed on a magnetic stirrer until homogenization and stored at 4°C. The stock of 10x transfer buffer was previously prepared by diluting the appropriate amount of Tris and Glycine in ddH2O to a final concentration of 0.25 M and 1.92 M, respectively.

Afterward, the migration buffer was poured-off the electrophoresis chamber, and the gel was released from the clamping frame and submerged in the transfer buffer. Next, the transfer sandwich was tightly assembled in the transfer buffer by placing the gel and the nitrocellulose membrane between the buffer-soaked blotting papers in this order: white cassette → sponge → two blotting papers → nitrocellulose membrane → gel → two blotting papers → black cassette, ensuring that no air bubbles were trapped between the gel and the membrane. Then, the assembled sandwich was placed in the transfer unit with the red side of the unit facing the white side of the cassette and the black side facing the black side of the cassette. Ice-cold 1x transfer buffer was then poured into the transfer cell and two ice blocks were added. The transfer cell was then closed with the lid and placed in a Styrofoam box covered with ice. We connected the transfer cell to the power supply and started the run at 350 mA (constant) and 150 V for one hour. Later, the membrane was placed in a Tupperware and covered with Panceau Red solution for one minute to visualize the transferred bands. Next, Panceau Red solution was poured-off and the membrane was washed couple of times with 0.3% TCA. This latter was prepared by diluting a stock of 10% TCA (Trichloroacetic acid, Cat. # T6399, Sigma) in ddH2O. Afterward, the membrane was submerged with 1x TBS-T washing buffer prior to membrane blocking. The 1x Tris buffered saline with

Tween (TBS-T) washing buffer was prepared by mixing 100 ml of 10x TBS with 900 ml of ddH2O and 1 ml of Tween 20, and then stirring them on a magnetic stirrer. The stock of 10x TBS solution was previously prepared by diluting powdered Tris and NaCl in ddH2O to a final concentration of 250mM and 1.5M, respectively. pH was then adjusted to 7.4 using concentrated HCl.

d. <u>Membrane Blocking and Antibody Incubation</u>

After protein transfer, the membrane was incubated in 5% non-fat dry milk prepared in 1x TBS-T to block the non-specific sites on the membrane. The incubation was performed on a shaker in the water bath at 37°C for 1 hour. Following blocking, the membrane was washed six times with 1x TBS-T on the shaker at room temperature, 5 minutes each. Next, the membrane was incubated in a plastic pouch with 5 ml of the primary antibody diluted in 5 ml of 1x PBS. Incubation was performed on the shaker in the cold room (at 4°C) overnight. The primary antibodies that we probed for in this study are: Rbm20 unconjugated rabbit polyclonal antibody provided at 1 µg/µl and used at 1:800 (bs-9606R, Bioss); and Notch2 (D76A6) XP, a rabbit monoclonal antibody provided at 515 µg/ml, and used at 1:1000 (5732S, Cell Signaling Technology). The next day, the membrane was washed six times with 1x TBS-T on the shaker at room temperature, 5 minutes each. Then, it was incubated in a plastic pouch with 5 ml of a Horseradish peroxidase (HRP)-conjugated secondary antibody diluted in 5 ml of 5% non-fat dry milk prepared in 1x TBS-T on the shaker at room temperature for 1 hour. The HRP-conjugated secondary antibody used in this study was goat anti-rabbit polyclonal IgG (H+L) provided at 0.8 µg/µl and used at 1:20000 (111-035-144, Jackson

Immunoresearch). After incubation with the secondary antibody, the membrane was washed with 1x TBS-T washing buffer at room temperature on the shaker for six times, 5 min each.

e. Imaging of Western Blots and Analysis of Results

Protein bands were detected using the western chemiluminescence substrate (Clarity^{TM} Western ECL Substrate, Cat. # 1705061, Bio-Rad), and the signal was using the ChemiDoc MP Imaging System (DTS facility, Bio-Rad). Results were analyzed and molecular weight of bands was determined using Image Lab software.

f. Membrane Stripping and Probing with a Different Primary Antibody

Antibodies bound to the membrane proteins were stripped using a stripping buffer that was previously prepared by diluting an appropriate amount of powdered glycine in ddH2O to a final concentration of 0.2 M, adding 0.1% of SDS, and 1% of Tween-20. The pH of the solution was adjusted to 2.2 using concentrated HCl. The membrane was incubated with the stripping buffer on a shaker at room temperature for 20 min. The stripping buffer was then discarded, and the membrane was washed twice with ~ 5 ml of 1x TBS-T on the shaker at room temperature, 5 min each. Afterward, the incubation step with the stripping buffer was repeated, followed by two washes with 1x TBS-T, 5 minutes each. Subsequently, the membrane was blocked in 5% non-fat dried milk prepared in 1x TBS-T as mentioned earlier on a shaker in the water bath at 37°C for 1 hour. This was followed by six washes with TBS-T washing buffer for 5 minutes each and incubation with 5 ml of a primary antibody (other than the one used before)

prepared in 1x PBS on a shaker in the cold room (at 4°C) overnight. We then proceeded as described previously.

4. Co-Immunoprecipitation

For this experiment, we used the Dynabeads® Co-Immunoprecipitation Kit (Cat. # 14321D, life technologies) containing Dynabeads® M-270 Epoxy as well as C1, C2, HB, LB and SB solutions.

a. Antibody-coupling

For the coupling of Notch2 antibody to magnetic beads, we weighed out 1.5 mg of Dynabeads® M-270 Epoxy in a 2 ml Ependorf. We also weighed out 1.5 mg of beads in another Ependorf for coupling with IgG antibodies that will serve as a negative control. All next steps were applied on both Eppendorfs. Next, we washed the beads with 1 ml of C1 solution and mixed them well by gentle pipetting up and down. The Ependorf was then placed on the previously disinfected magnet (Cat. # 12321D, Thermo Fisher Scientific) for 1 min so the beads collect at the tube wall, then we removed the supernatant. Magnetic beads were re-suspended with 46 µl of C1 and 29 µl of Notch2 primary antibody, then mixed well by gentle pipetting. The antibody used in this study was Notch2 (D76A6) XP, a rabbit monoclonal antibody provided at 515 µg/ml (5732S, Cell Signaling Technology). For the negative control tube, we added 57.5 µl of C1 and 17.5 µl of IgG antibody, and mixed well. Afterward, we added 75 µl of C2 to each tube and mixed well. Finally, we swirled the tubes couple of times to set a limit for the movement of the solution and incubated on a roller at 37°C overnight (16-24 hours).

The next day, we placed the tubes on the magnet for 1 min, allowed the beads to collect at the tube wall, and then removed the supernatant. Next, we washed the beads with 800 µl of HB solution and placed the tubes again on the magnet for 1 min, then removed the supernatant. Magnetic beads were next washed with 800 µl of LB solution, placed on the magnet for 1 min, and then the supernatant was discarded. Following LB wash, we washed the beads twice with 800 µl of SB solution, each followed by placing the tubes on the magnet for 1 min and supernatant removal. Afterward, we did one long SB wash, where we added 800 µl of SB solution to each tube, mixed well, and incubated on a roller at room temperature for 15 min. The tubes were placed on the magnet for 1 min and the supernatant was removed. Finally, we re-suspended the antibody-coupled beads with 150 µl of SB solution and stored them in the fridge at 4°C.

b. Protein Extraction and Cell Sample Preparation

RD cells were seeded in four T-175 flasks in 20 ml of complete growth medium each (Cat. # D6429, Sigma-Aldrich). When cells reached 100% confluence in culture, they were washed once with pre-cooled PBS (1x) using 10 ml/T-175 flask. This was followed by the addition of 4 ml of Trypsin-EDTA per flask to detach the cells from the surface of the T-175 flask post incubation at 37°C and 5% CO2 for 30 sec. Cells were then re-suspended in 12 ml of complete growth medium to inactivate trypsin. Next, the content of each T-175 flask was transferred to a separate pre-weighed 15 ml conical tube and centrifuged at 200xg for 5 min at 4°C. Supernatant was discarded and cells were washed twice with 2 ml of pre-cooled PBS, each followed by a centrifugation at 200xg for 5 min at 4°C. Afterward, we removed as much liquid as possible from the

cells and weighed the tubes again to calculate the weight of cell pellets. Next, cells were

re-suspended with an appropriate volume of extraction buffer on ice depending on the

cell mass (1:9 ratio of cell mass/extraction buffer). The extraction buffer was freshly

prepared by mixing 4 ml of 1x IP solution with 10 µl (1:400) of protease inhibitor

cocktail and 10 µl of Phosphatase inhibitor cocktail II (Cat.# L41600092-1,

bioWORLD). The protease inhibitor cocktail was prepared by mixing 6 µl of PMSF, 3

µl of Benzamidine, 6 µl of Leupeptin, 3 µl of Aprotinin, and 20 µl of Na

pyrophosphate. Next, we incubated with the extraction buffer on ice for 15 min,

vortexing halfway through. Finally, we centrifuged the cells at 2600xg for 5 min at 4°C

to remove large cell debris and nuclei, and transferred all supernatants to one common

fresh pre-cooled tube placed on ice. Extracted proteins were immediately used for the

Co-Immunoprecipitation assay.

c. Co-Immunoprecipitation of Proteins

    After protein extraction from RD cells, 60 µl of the proteins-containing solution

were transferred to a new Ependorf and placed in the freezer at -20°C. This served as a

positive control later on. Next, the antibody-coupled beads were transferred to fresh

tubes, which were placed on the magnet for 1 min for the beads to collect at the tube

wall. Supernatant was discarded and 400 µl of 0.01% BSA in 1x PBS was added to each

of the tubes. Tubes were then rotated for 5 min on a rotator at room temperature and

placed on the magnet for 1 min for supernatant removal. Afterward, Dynabeads were

washed with 900 µl of extraction buffer that was freshly prepared as mentioned

previously. Tubes were placed on the magnet for 1 min and supernatant was removed.

Then, we resuspended the Notch2 and IgG-coupled beads with equal amounts of cell lysates and incubated for 1 hour on a roller at 4°C. Following incubation, tubes were placed on the magnet and the supernatant containing unbound proteins was removed. Then, the beads were washed with 200 µl of extraction buffer thrice, two quick washes and one last 5 minutes wash. After each wash, tubes were placed on the magnet and supernatant was removed. Next, beads were washed one more time with 200 µl of 1x LWB (last wash buffer), mixed by gentle pipetting, and incubated on a roller at room temperature for 5 min. The 1x LWB solution was prepared by diluting 200 µl of 5x LWB in 800 µl of ddH2O and then adding 0.2 µl of Tween-20 (0.02%). After these washing steps, the beads solution was transferred to clean pre-labeled tubes, which were next placed on the magnet for 1 min to remove the LWB solution. Afterward, beads were re-suspended in 60 µl of EB (elution buffer) solution and incubated on a roller at room temperature for 5 min. Finally, the beads-containing tubes were placed on the magnet for 1 min for the beads to collect at the tube wall, and the supernatant containing the purified proteins was transferred to a fresh tube. This solution was then used in Western Blotting for proteins' visualization.

d. Western-Blotting

Co-Immunoprecipitation results were read and analyzed using Western Blotting where we followed the same steps as mentioned earlier in this manuscript. The only differences were in the protein preparation and protein loading steps. Once the purified protein complex were collected after co-immunoprecipitation, 15 µl of 4x Laemmli was added to both Notch2 and negative control tubes as well as the positive control tube that

was stored at -20°C earlier in this experiment. All tubes were then vortexed and placed on a pre-heated heat block (95°C) for 10 min for proteins denaturation. For the protein loading step, samples were spinned down for ~ 1 min then loaded slowly and vertically in the gel wells. In this experiment, we used the 10 wells, 1.5 mm thick comb. Created wells were filled with protein ladder, positive controls, negative control and our sample as following. The first well was loaded with 4 µl of the Tricolor Broad Protein Ladder (Cat. # BR0900101, biotechrabbit). The second well was loaded with 25 µl, the third with 15 µl and the fourth with 10 µl of the positive control solution. These three wells served as high, moderate, and low input consecutively. The fifth well was loaded with 55 µl of the negative control solution in which IgG antibodies were coupled to Dynabeads. Finally, 55 µl of the protein sample, where Notch2 antibodies were coupled to beads, was loaded in the sixth well. After protein loading, SDS-PAGE was ran at 200 V until the blue tracking dye reached the bottom of the gel. The rest of the steps were the same as described previously in the SDS-PAGE section of this manuscript.

CHAPTER III

RESULTS

A. Assess the expression and the intracellular distribution of Notch2 protein, and determine if it co-localizes with RBM20 protein using immunofluorescence staining.

1- Paraformaldehyde (PFA) fixation method is not compatible with the staining of RBM20 and Notch2 proteins in RD cells.

RBM20	**Primary Ab**	Goat polyclonal IgG, Santa Cruz
	Secondary Ab	Alexa-Fluor 488 donkey anti-goat
Notch2	**Primary Ab**	Rabbit monoclonal Ab, Cell Signaling
	Secondary Ab	Alexa-Fluor 647 donkey anti-rabbit
Fixation method		PFA
Mounting medium		Ultra-Cruz^{TM} Hard-Set
Co-staining of RBM20 and Notch2		Yes
Microscope		Upright fluorescent microscope

Table 6 | Summary of experimental conditions for IF staining where PFA was used for the fixation of RD cells.

We aimed to determine the intracellular distribution of RBM20 and Notch2 proteins, and whether they co-localize inside of RD cells, indicating a possible protein-protein interaction. For this purpose, Immunofluorescence (IF) staining experiments were performed on RD cells where many optimization steps were done and multiple fixation methods were used.

First, we used the Paraformaldehyde fixation method for the IF staining of RD cells. For RBM20 protein, we used the Rbm20 goat polyclonal IgG provided by Santa Cruz Biotechnology as a primary antibody and Alexa Fluor 488 donkey anti-goat as the

secondary antibody, staining the protein in green. On the other hand, for Notch2 protein, we used the Notch2 rabbit monoclonal antibody by Cell Signaling Technology as a primary antibody, and Alexa Fluor 647 donkey anti-rabbit as the secondary antibody, giving a far-red color.

After microscopic imaging using the upright fluorescent microscope (CRSL core lab), results were not satisfying where RD cells barely appeared. Also, neither DAPI staining of the nuclei nor RBM20 and Notch2 proteins were observed clearly and stained properly (Figure 11). These results indicated that the PFA fixation method is not compatible for RD cells.
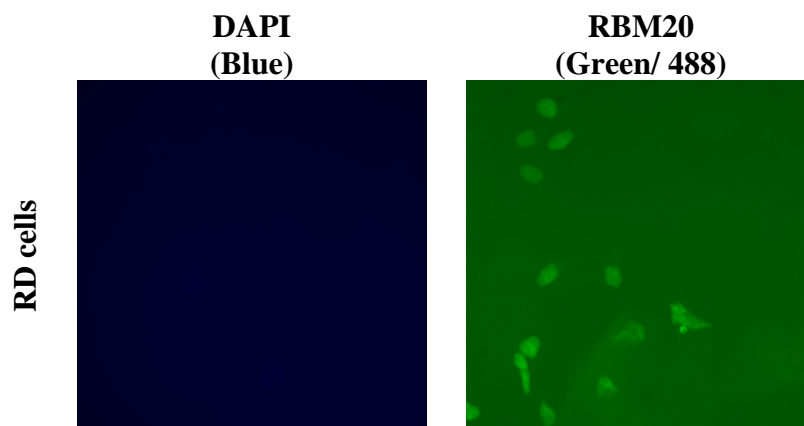
Figure 11 | Immunofluorescence co-staining of RBM20 and Notch2 proteins in RD cells, where PFA was used for fixation. Representative microscopic images using the upright fluorescent microscope showing an unsuccessful staining of these proteins. DAPI was used to stain the nuclei (blue). RBM20 and Notch2 proteins were stained in green (Alexa Fluor 488) and far-red (Alexa Fluor 647), respectively. Images were acquired at 40x magnification.

2- Acetone-Methanol fixation method is compatible for the staining of RBM20 and Notch2 proteins in RD cells, and Notch2 unconjugated primary antibody is better that the pre-conjugated one.

RBM20	Primary Ab	Goat polyclonal IgG, Santa Cruz
	Secondary Ab	Alexa-Fluor 488 donkey anti-goat
Notch2	Primary Ab	Rabbit monoclonal Ab, Cell Signaling
	Secondary Ab	Alexa-Fluor 647 donkey anti-rabbit
Fixation method		Acetone-methanol
Mounting medium		Ultra-Cruz™ Hard-Set
Co-staining of RBM20 and Notch2		Yes
Microscope		Upright fluorescent microscope

Table 7 | Summary of experimental conditions for IF staining where RD cells were fixed with acetone and methanol, and Notch2 unconjugated primary antibody was used.

RBM20	Primary Ab	Goat polyclonal IgG, Santa Cruz
	Secondary Ab	Alexa-Fluor 488 donkey anti-goat
Notch2	Primary Ab	Rabbit pre-conjugated to Alexa Fluor 647
	Secondary Ab	X
Fixation method		Acetone-methanol
Mounting medium		Ultra-Cruz™ Hard-Set
Co-staining of RBM20 and Notch2		Yes
Microscope		Upright fluorescent microscope

Table 8 | Summary of experimental conditions for IF staining where RD cells were fixed with acetone and methanol, and Notch2 pre-conjugated primary antibody was used.

Next, we intended to use the acetone-methanol fixation method to fix RD cells for IF staining. For RBM20 proteins, we used the same primary and secondary antibodies as before. However, for Nocth2 proteins, we used the unconjugated primary antibody by Cell Signaling Technology in one trial, and the pre-conjugated antibody in another trial. We imaged the slides on the upright fluorescent microscope.

Results showed better visualization of RD cells, their nuclei and RBM20 proteins. Nevertheless, Notch2 proteins were only visualized when the unconjugated Notch2 primary antibody was used (Figure 12). These results indicated that the acetone-methanol fixation method is more suitable for RD cells, and that Notch2 unconjugated primary antibody is better than the pre-conjugated one. Although RD cells appeared better using this fixation method and the mentioned unconjugated Notch2 primary antibody, RBM20 proteins were not as clear, where they were not visualized as individual clear dots, indicating the need for further optimizations.
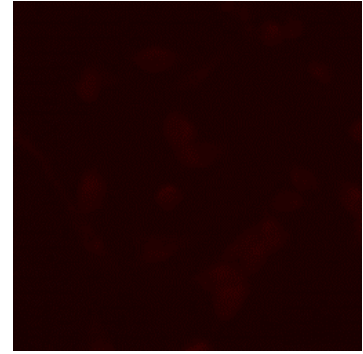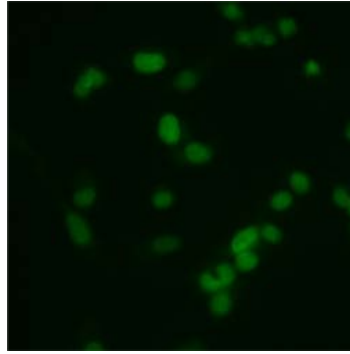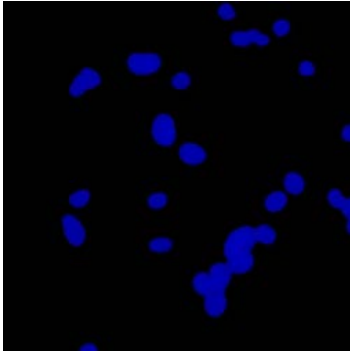
A)

| DAPI (blue) | RBM20 (green/ 488) | Notch2 (Pre-conjugated Ab) (Far-red/ 647) |

RD cells

B)

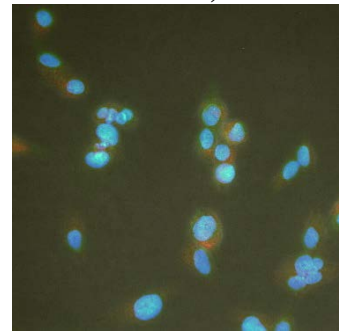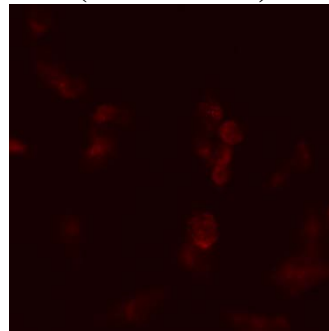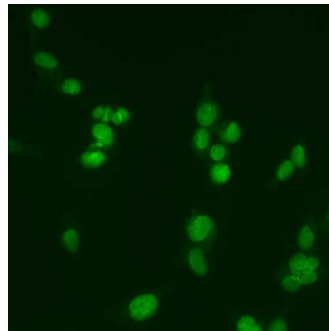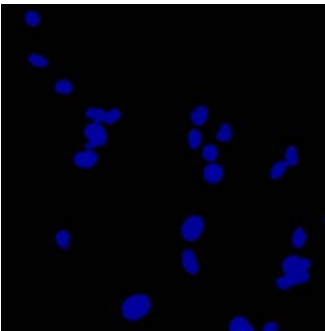| DAPI (Blue) | RBM20 (green/ 488) | Notch2 (Unconjugated Ab) (Far-red/ 647) | Overlay (RBM20 + Notch2 + DAPI) |

RD cells

Figure 12 | Immunofluorescence co-staining of RBM20 and Notch2 proteins in RD cells where the acetone-methanol method was used for fixation. Representative microscopic images of Notch2 and RBM20 proteins which were stained in far-red (Alexa Fluor 647) and green (Alexa Fluor 488), respectively. DAPI was used to stain the nuclei in blue. **Panel A;** Notch2 primary antibody was pre-conjugated to a fluorophore and no secondary antibody was used. **Panel B;** Notch2 primary antibody was unconjugated to a fluorophore, and a corresponding Alexa Fluor-conjugated secondary antibody was used. Results showed a better staining of RD cells using the acetone-methanol method, and a better staining of Notch2 protein in specific using the unconjugated primary antibody. In this assay, the upright fluorescent microscope was used for imaging, and images were acquired at 40x magnification.

3- Notch2 proteins are distributed mainly in the cytoplasm, but also present in the nuclei of RD cells.

RBM20	**Primary Ab**	Goat polyclonal IgG, Santa Cruz
	Secondary Ab	Alexa-Fluor 647 donkey anti-goat
Notch2	**Primary Ab**	Rabbit monoclonal Ab, Cell Signaling
	Secondary Ab	Alexa-Fluor 488 donkey anti-rabbit
Fixation method		Acetone-methanol
Mounting medium		Ultra-Cruz^{TM} Hard-Set
Co-staining of RBM20 and Notch2		Yes
Microscope		Confocal microscope

Table 9 | Summary of experimental conditions for IF staining where Notch2 proteins were stained in green and RBM20 proteins were stained in far-red. Also, confocal microscope was used for imaging.

After being able to fix RD cells efficiently using the acetone-methanol method, we aimed to optimize the secondary antibodies used for RBM20 and Notch2. Therefore, in this co-localization IF assay, while using the same RBM20 primary antibody provided by Santa Cruz Biotechnology, we used a different secondary antibody which was the Alexa Fluor-647 donkey anti-goat IgG, enabling the visualization of the protein in far-red. Also, we used the unconjugated Notch2 primary antibody by Cell Signaling

58

Technology, and the Alexa Fluor-488 donkey anti-rabbit IgG as a secondary antibody,

staining the protein in green. Slides were imaged using the confocal microscope (DTS

facility). In this trial, Notch2 proteins, stained in green, appeared beautifully with a

distribution in both the nucleus and the cytoplasm of RD cells. Notch2 proteins were

found to be mostly localized in the cytoplasm of RD cells, yet they were also present in

the nuclei of the cells (Figure 13 A). However, RBM20 proteins did not appear in these

slides, hindering us from taking a clear indication on the co-localization of RBM20 and

Notch2 proteins. Furthermore, RD cells were sometimes found to be under a viscous

solution that we believed it was because of the mounting medium used (Figure 13 B).

Thus, this mounting medium had to be used in a decreased quantity or even substituted

with another one.

A)

B)
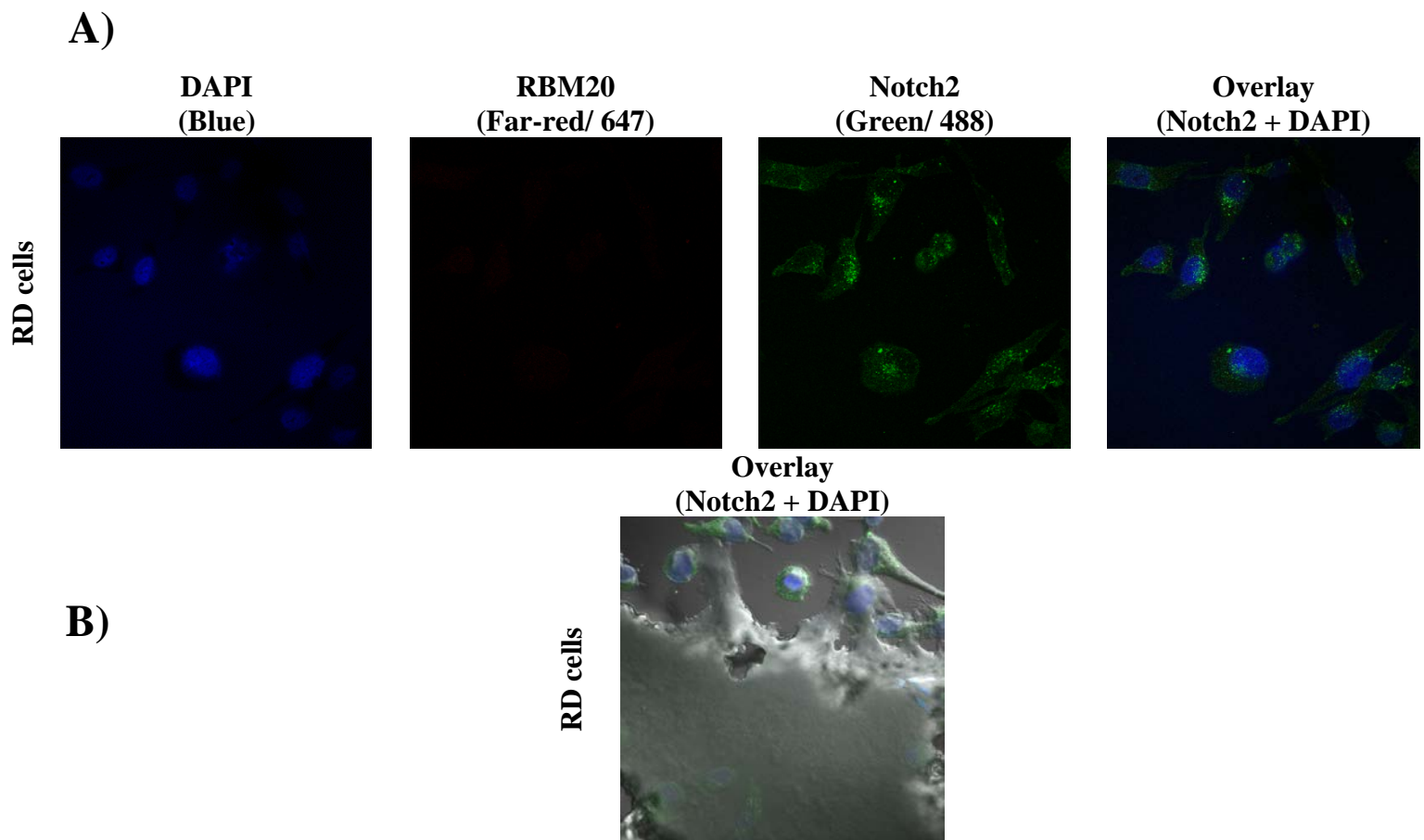
Figure 13 | Immunofluorescence staining of RBM20 and Notch2 proteins in RD cells where the acetone-methanol method was used for fixation. RBM20 proteins were colored in red (Far-red color, Alexa Fluor-647), whereas Notch2 proteins were colored in green (Alexa Fluor-488). **Panel A;** Representative microscopic images using the confocal microscope showing the distribution of Notch2 proteins which were mainly in the cytoplasm of RD cells, with a fewer distribution in the nuclei. RBM20 proteins did not appear. DAPI was used to stain the nuclei. Images were acquired at 63x magnification. **Panel B;** representative confocal microscopy image showing RD cells hided under the mounting medium.

**4- RBM20 protein is primarily localized in the nucleus, but is also found in the cytoplasm of RD cells**.

a. RBM20 unconjugated rabbit primary antibody (Bioss) works well for the staining of RBM20 proteins in RD cells.

RBM20	Primary Ab	Rabbit polyclonal Ab, Bioss
	Secondary Ab	Alexa-Fluor 647 donkey anti-goat
Notch2	Primary Ab	Rabbit monoclonal Ab, Cell Signaling
	Secondary Ab	Alexa-Fluor 647 donkey anti-rabbit
Fixation method		Acetone-methanol
Mounting medium		Ultra-Cruz^{TM} Hard-Set
Co-staining of RBM20 and Notch2		No
Microscope		Confocal microscope

Table 10 | Summary of experimental conditions for IF staining where RBM20 anti-rabbit primary antibody was used. Also, RBM20 and Notch2 proteins were stained separately.

After being able to clearly visualize Notch2 proteins inside of the RD cells, we aimed to optimize our next experiment in order to visualize and determine the localization and intracellular distribution of RBM20 proteins. Although the RBM20 primary antibody provided by Santa Cruz Biotechnology was working well and yielding good results, we were obliged to use a new antibody because of the shortage on that previously used one. The new antibody that we used was the Rbm20 unconjugated rabbit polyclonal antibody by Bioss Company. Also, we were short on the donkey anti-rabbit Alexa Fluor-488 secondary antibody that worked perfectly with the Notch2 rabbit primary antibody before. Thus, we used the donkey anti-rabbit Alexa Fluor-647 that was used early on for the IF experiment. In addition, because the new RBM20 primary

antibody is raised in rabbits similar to our Notch2 primary antibody, we were unable to do co-localization assays. Therefore, we stained RBM20 and Notch2 proteins separately in this trial. Microscopic imaging was done using confocal microscopy (DTS facility). After imaging of the slides, RBM20 proteins appeared beautifully, being distributed in both the nuclei and cytoplasm of RD cells, with a prevalent localization in the nucleus compartment. Also, Notch2 proteins were clearly visualized and distributed mainly in the cytoplasm, but also present in the nuclei of RD cells (Figure 14). Despite using a fewer amount of the mounting media, some of the cells were hided under the mounting solution, indicating the necessity of using a different mounting medium.

A)

Overlay
RBM20 (Far-red/ 647) + DAPI (Blue)

B)

Overlay
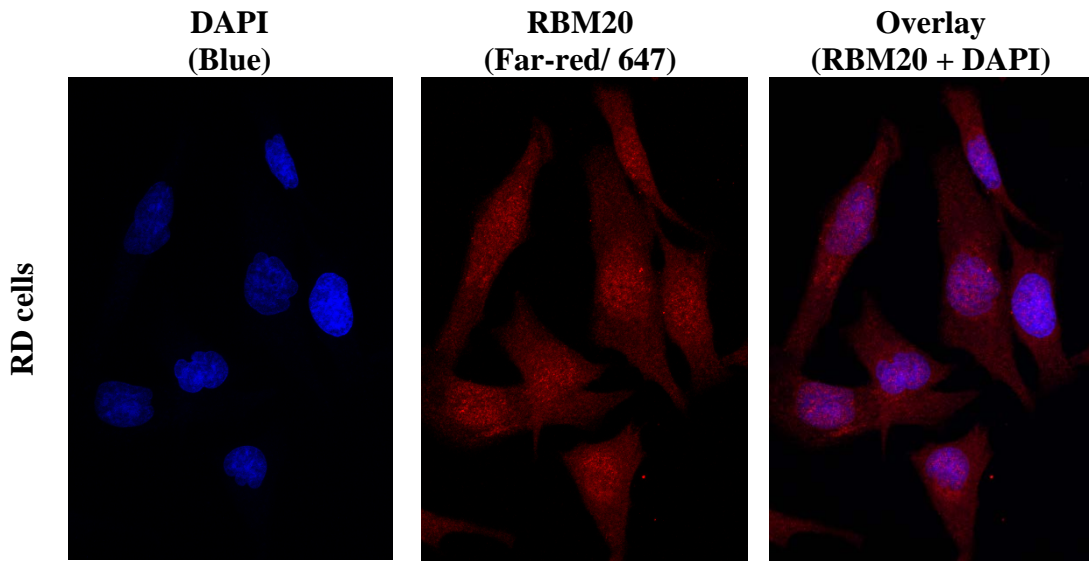**Notch2 (Far-red/ 647) + DAPI (Blue)**
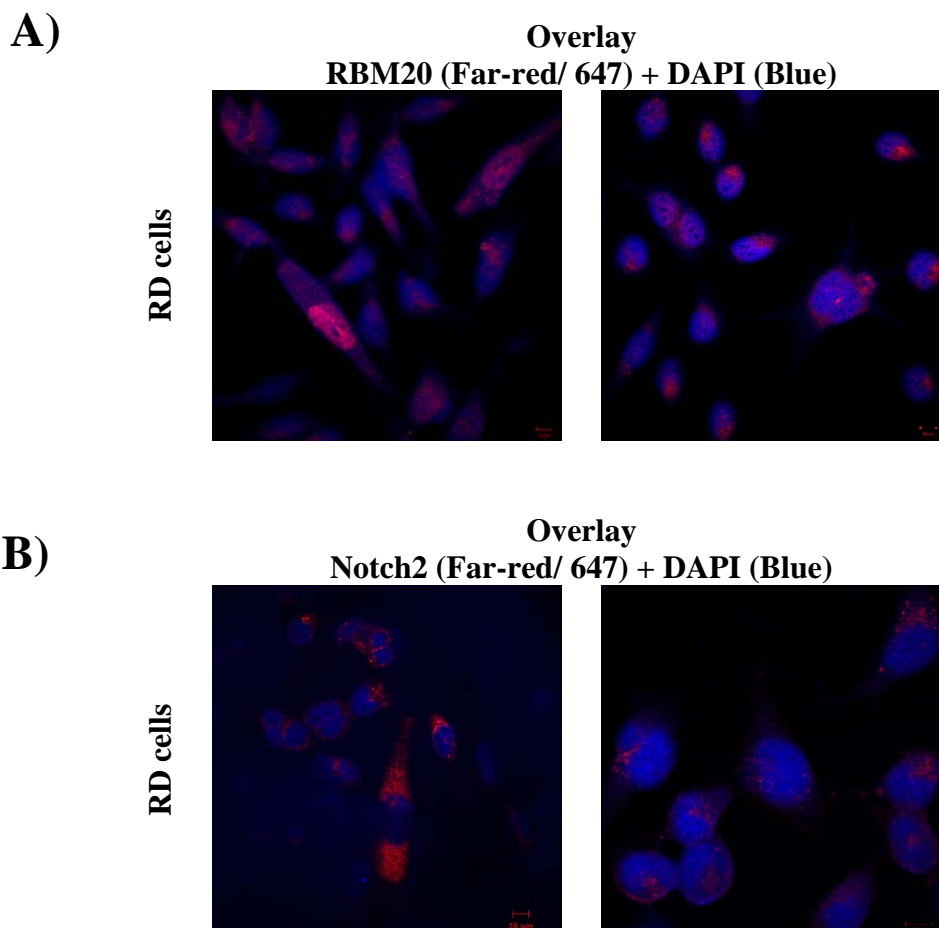
Figure 14 | Immunofluorescence staining of RBM20 and Notch2 proteins in RD cells where the acetone-methanol method was used for fixation. RBM20 and Notch2 proteins were stained separately with the same secondary antibody (Far-red color, Alexa Fluor-647). Representative microscopic images using the confocal microscope showing the distribution of RBM20 proteins mainly in the nuclei of RD cells, with a fewer distribution in the cytoplasm (**Panel A**). Also, Notch2 proteins were shown to be distributed mostly in the cytoplasm, but also present in the nuclei of RD cells (**Panel B**). DAPI was used to stain the nuclei in blue. Images were acquired at 63x magnification.

b. <u>ProLong^{TM} Gold antifade mounting medium is better that the previously used Ultra-Cruz^{TM} Hard-Set mounting medium</u>.

RBM20	**Primary Ab**	Rabbit polyclonal Ab, Bioss
	Secondary Ab	Alexa-Fluor 647 donkey anti-goat
Notch2	**Primary Ab**	X
	Secondary Ab	X
Fixation method		Acetone-methanol
Mounting medium		ProLong^{TM} Gold antifade reagent
Co-staining of RBM20 and Notch2		No
Microscope		Confocal microscope

Table 11 | Summary of experimental conditions for IF staining where RBM20 proteins were stained in far-red. Also, ProLong^{TM} Gold antifade reagent was used as mounting medium.

In the next trial, we used the ProLong^{TM} Gold antifade mounting medium, which enabled us to visualize a clear distribution of the RBM20 proteins inside of the cells. As previously mentioned, RBM20 proteins were found to be massively present in the nuclei of RD cells, and present in fewer amount in the cytoplasm of these cells (Figure 15).

| | DAPI
(Blue) | RBM20
(Far-red/ 647) | Overlay
(RBM20 + DAPI) |

Figure 15 | Immunofluorescence staining of RBM20 proteins in RD cells where the acetone-methanol method was used for fixation. RBM20 proteins were colored in far-red (Alexa Fluor-647). Representative microscopic images using the confocal microscope showing the distribution of RBM20 proteins mainly in the nuclei of RD cells, with a fewer distribution in the cytoplasm. DAPI was used to stain the nuclei. Images were acquired at 63x magnification.

5- Analysis of the distribution of RBM20 and Notch2 proteins inside the different cellular compartments of RD cells after IF staining.

Acquired images from the confocal microscope were analyzed by subjective assessment of the subcellular localization of RBM20 and Notch2 proteins. This was done by counting the number of cells in each frame and determining the distribution of the proteins of interest inside the different RD cells in each of these frames according to the location of the nuclei colored in blue. Our results showed that 80.6 % of RD cells were expressing RBM20 proteins in both the nucleus and the cytoplasm with a higher expression in the nucleus. In 17.2 % of these cells, RBM20 proteins were distributed mostly in the cytoplasm, but also present in fewer amounts in the nucleus. In addition, a minority of RD cells expressed RBM20 proteins solely in the nucleus or the cytoplasm,

where these accounted for only 1.4 % and 0.8 % of counted cells respectively. (Figure 16). As for Notch2 proteins' subcellular distribution, 59.5 % of RD cells expressed these proteins in both the nuclear and cytoplasmic compartments, with a higher expression in the cytoplasm compared to the nucleus. Also, Notch2 proteins were expressed solely in the cytoplasm of 30 % of RD cells. Moreover, although 10.3 % of imaged cells showed a higher expression in the nucleus with a fewer expression in the cytoplasm, yet none of RD cells expressed Notch2 proteins solely in the nucleus. (Figure 16)
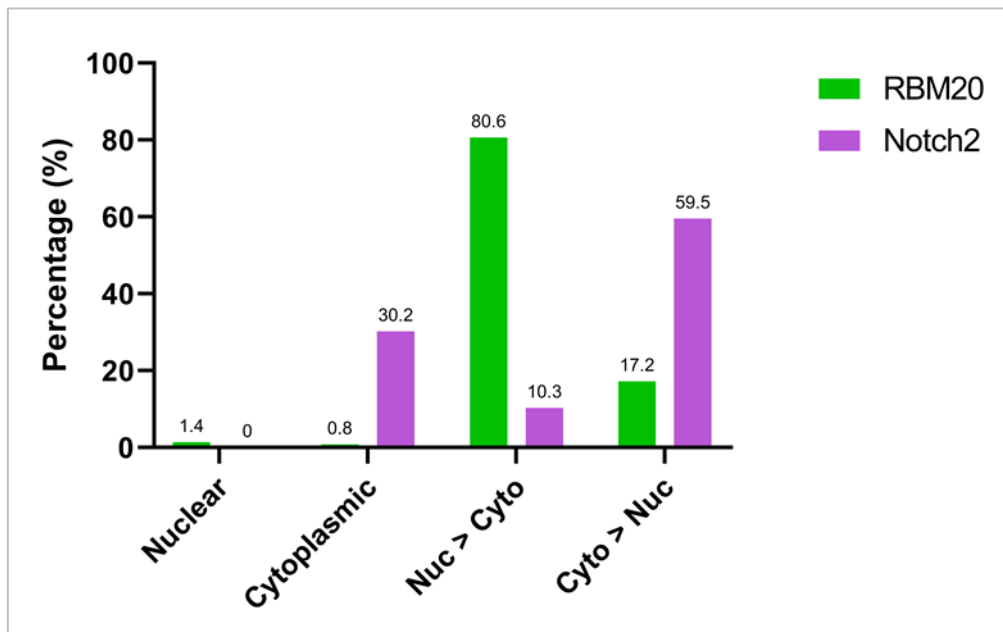
Figure 16 | Assessment of the subcellular localization of RBM20 and Notch2 proteins revealed a distribution of RBM20 proteins in both the cytoplasmic and nuclear compartments of 97.8 % of stained RD cells. Similarly, Notch2 proteins were co-expressed in both the cytoplasmic and nuclear compartments of 69.9 % of stained RD cells. Data were plotted using GraphPad Prism 8.

B. Determine whether there is a direct interaction between RBM20 and Nocth2 proteins, using Co-Immunoprecipitation.

1. **Notch2 protein appears at ~ 106 KDa on Western Blotting performed on proteins extracted from RD cells, whereas two isoforms of RBM20 appear on the blot, one having a molecular weight of ~ 125 KDa and the other one of ~ 45 KDa.**

Prior to performing the Co-Immunoprecipitation assay, we aimed to optimize the Western Blotting of RD cells, and to determine the molecular weights of Notch2 and RBM20 proteins, as well as the isoforms expressed in this cell line. To this end, Western Blotting experiments were executed on RD cells post protein extraction and protein quantification. Under baseline conditions, western blotting results revealed that RD cells express two isoforms of the RBM20 protein, one of ~125 KDa and the other one of ~ 45 KDa (Figure 17), where the lower molecular weight isoform represents approx. 89 % of the total RBM20 volume, whereas the isoform having the higher molecular weight accounts for 11 % of the total volume as determined by the densitometry analysis using Image Lab software. Also, results showed that RD cells express Notch2 protein having a molecular weight of ~ 106 KDa. (Figure 18)
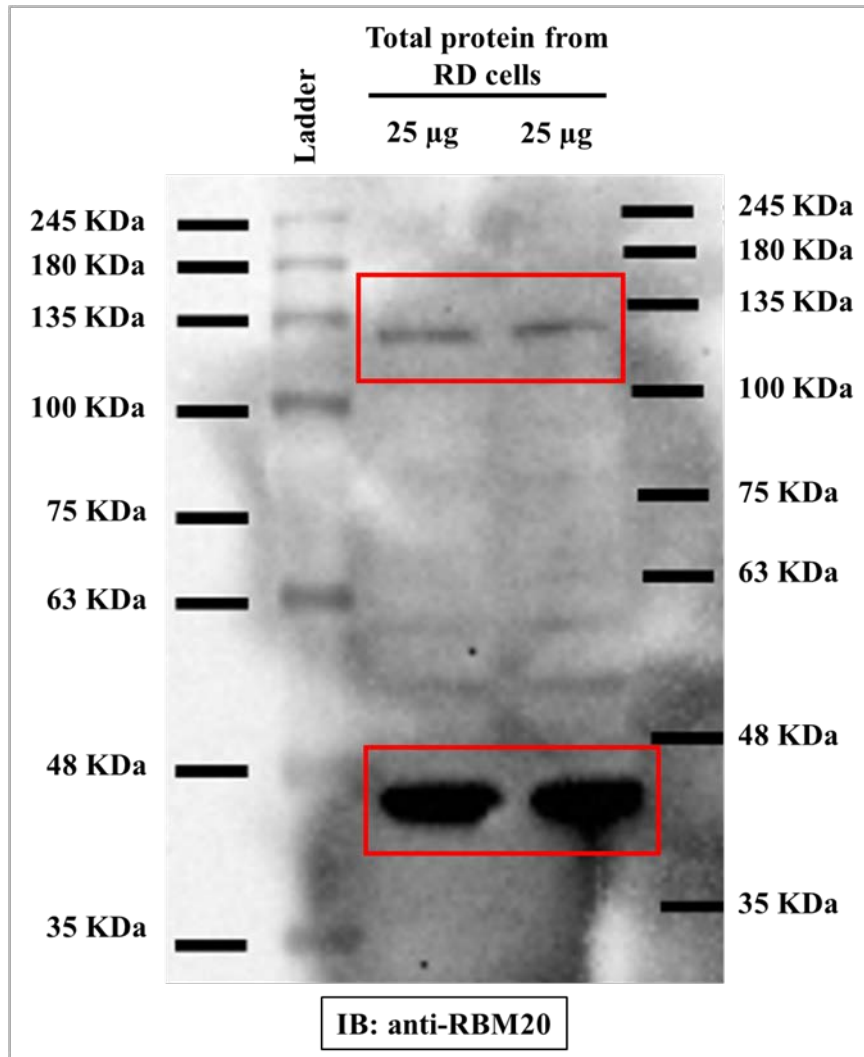
Figure 17 | Representative blot of the western blotting analysis of RBM20 expression in RD cells cultured at full confluence under baseline conditions. Two isoforms of RBM20 appeared, one at ~ 125 KDa, and the other one at ~ 45 KDa. Abbreviations: **IB**, ImmunoBlot.
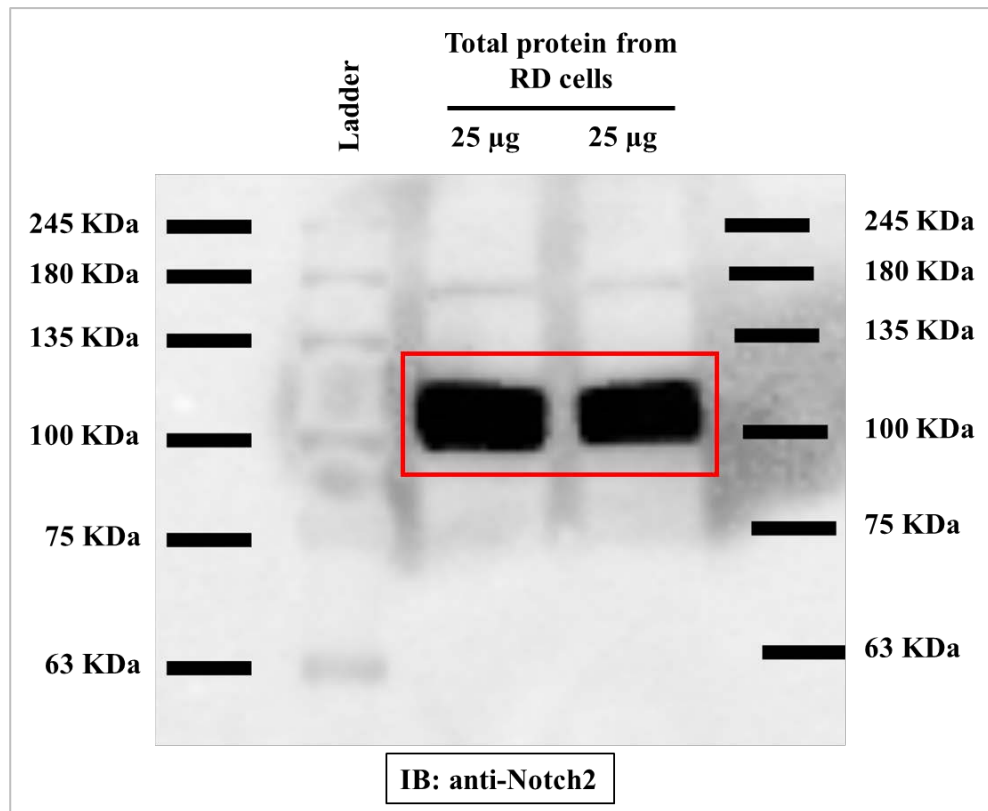
Figure 18 | Representative blot of the western blotting analysis of Notch2 expression in RD cells cultured at full confluence under baseline conditions. Notch2 protein appeared at ~ 106 KDa. Abbreviations: **IB**, ImmunoBlot.

2. Notch2 pulls down RBM20 protein in the Co-Immunoprecipitation assay

In the second aim of this study, we intended to test whether there is direct protein-protein interaction between RBM20 and Notch2 proteins. Thus, we executed Co-Immunoprecipitation experiment on RD cells' protein extract when cells were cultured at full confluence under baseline conditions. Accordingly, we first coupled Notch2 antibodies to magnetic Dynabeads and subjected the obtained antibody-coupled beads to RD cells' protein lysate containing RBM20 and Notch2 proteins in their physiological state. Beads coupled to Notch2 protein complex were next purified and blotted using SDS-PAGE. Interestingly, results of this assay revealed the presence of

RBM20 protein having a molecular weight of ~ 129 KDa among the protein complex

bound to Notch2 protein. (Figure 19) However, shortage in some of necessary reagents

hindered us from repeating and validating these findings in further Immunoprecipitation

assays.
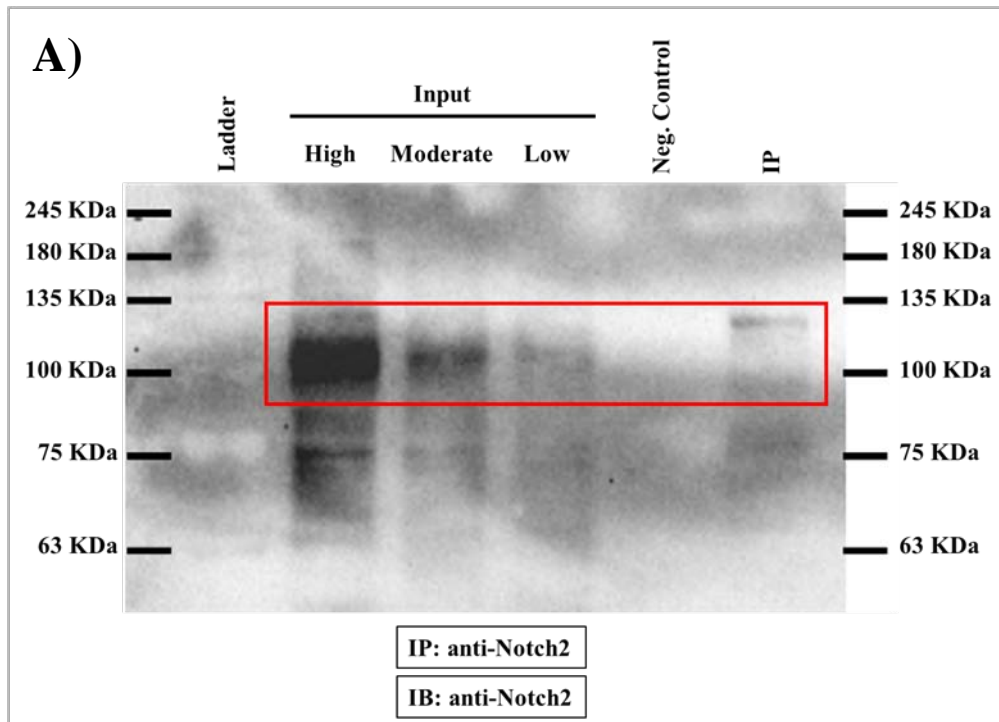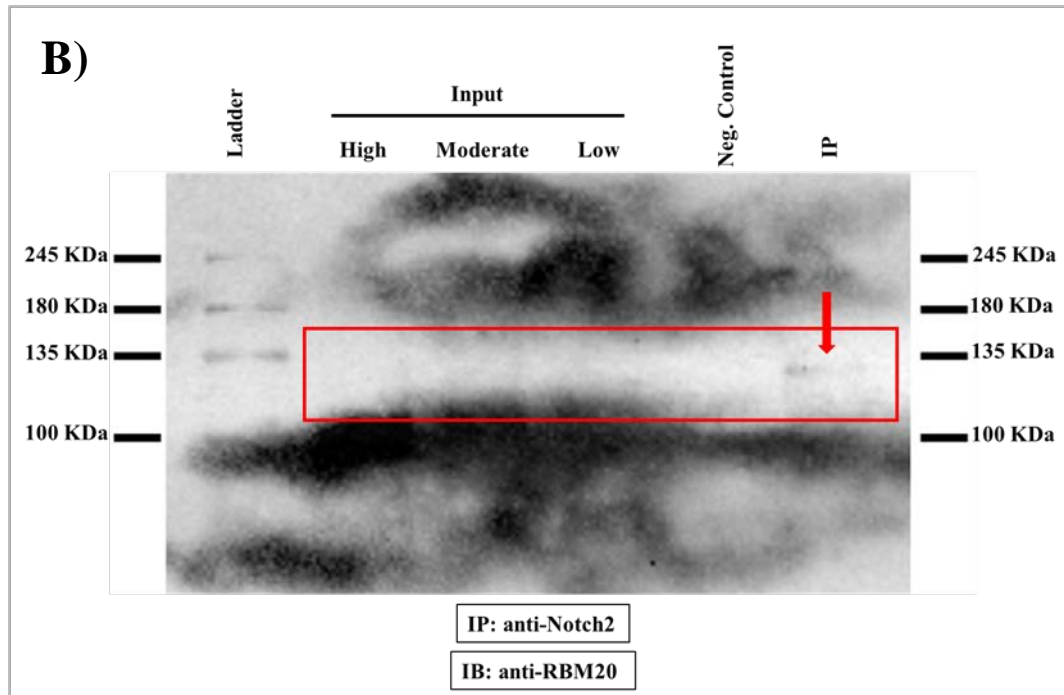
Figure 19 | Western Blotting analysis showing Co-Immunoprecipitation results where Notch2 antibodies were coupled to magnetic beads. RBM20 was tested for being among the eluted proteins that were pulled down by Notch2 protein. **Panel A;** Representative blot probed with Notch2 antibody where bands appeared in lanes 2, 3, 4 and 6 with molecular weights of approx. 111, 106,106 and 122 KDa. **Panel B;** Representative blot probed with RBM20 antibody where a band of ~129 KDa appeared in lane 6.

CHAPTER IV

DISCUSSION

Dilated Cardiomyopathy (DCM) is a disease of the myocardium characterized by the dilatation and enlargement of the left ventricle, causing weakening of the heart and ultimately leading to heart failure and sudden cardiac death. Estimates suggest that up to one-third of individuals with DCM have familial disease. One of the newly discovered mutations causing DCM affects the function of RBM20, a member of the Serine/Arginine-rich protein family that regulates and selects alternative splicing sites in eukaryotic pre-mRNA. In light of its recent discovery, and the fact that not much is known about the biofunctional relevance of *RBM20* gene product and its putative interacting partners, *RBM20* was the focus of our study. In particular, our interest was to study the potential protein-protein interaction between RBM20 and Notch2 proteins. The choice of Notch2 was based on our phage display biopanning assay findings, where Notch2 protein was identified among the putative interacting partners with RBM20. As such, we rationalized that there is an interaction between RBM20 and Notch2 proteins in healthy heart cells and that the Dilated Cardiomyopathy disease arising due to mutations in the *RBM20* gene is mediated in part by a disruption of the interaction between the RBM20 and Notch2 proteins.

Immunofluorescence staining of RD (Rhabdomyosarcoma) cells cultured at 80% confluence shows that RBM20 proteins are mainly localized in the nuclei of RD

(Rhabdomyosarcoma) cells, but they are also expressed in the cytoplasm of these cells. In terms of numbers, 97.8% of counted RD cells expressed RBM20 proteins in both the nuclear and cellular compartments. Besides, Notch2 proteins were found to be most prominently distributed in the cytoplasmic compartment of RD cells, but also present in the nuclei, where 59.5% of counted RD cells expressed Notch2 proteins in both the nucleus and the cytoplasm of RD cells. However, it is important to mention that after the optimization of the Immunofluorescence staining assay, we were unable to co-localize RBM20 and Notch2 proteins by co-staining them since the antibodies of both proteins were raised in the same animal species (rabbit).

Despite the fact that co-localization of RBM20 and Notch2 proteins in the same cellular compartment, being the nucleus or the cytoplasm, does not guarantee or prove an interaction between these two proteins in human hearts especially because we are using a cancerous striated muscle cell line, however, this piece of information represents a promising preliminary finding that needs to be further confirmed using other laboratory techniques highlighting protein-protein interactions in heart-derived cell lines and heart tissue. Expression of both RBM20 and Notch2 proteins in the cytoplasm and nuclei of RD cells proposes an interaction between these two proteins by binding to each other inside and/or outside the nucleus where RBM20 exerts its activity by affecting splicing of target mRNAs.

Our next aim was to assess the direct interaction between RBM20 and Notch2 proteins by performing Co-Immunoprecipitation (Co-IP) assays. Thus, prior to this, we intended to determine the molecular weights of the RBM20 and Notch2 proteins

expressed in RD cells. Western blotting analyses revealed the expression of two RBM20 isoforms, having ~125 KDa and ~ 45 KDa, and Notch2 protein of ~106 kDa. The importance of these findings falls in the analysis and accurate interpretation of the Co-IP results. Next, we performed Co-Immunoprecipitation assay followed by Western Blotting for the detection of precipitated proteins and analysis of the results. Molecular weight analysis of purified proteins revealed the presence of RBM20 among the proteins that were pulled down by Notch2, suggesting a protein-protein interaction between RBM20 and Notch2 proteins, favoring our hypothesis of a potential interplay between them. However, this assay was executed for one single time; thus, it needs to be repeated in order to validate these results. Also, our western blots visualized after Co-Immunoprecipitation have a high background, which limited our ability to analyze the results and interpret them in the best way, highlighting the need for further optimizations and repeats.

To sum up, conclusions drawn from the Immunofluorescence and Co-Immunoprecipitation assays support our hypothesis and promise of a protein-protein interplay between RBM20 and Notch2 proteins that might explain in part the development of Dilated Cardiomyopathy disease in case of mutations or down-regulation of the *RBM20* gene.

As per our plan, Co-Immunoprecipitation assays will be replicated on RD cells as well as left ventricular heart tissue derived from healthy male rats granted by Dr. Assad Eid. This will give us a better understanding, and stronger evidence of the protein-protein interplay between RBM20 and Notch2 proteins as these are fresh,

healthy cells, mimicking human cardiac cells. Also, Proximity Ligation Assays (PLA) will be performed on RD and H9c2 cells, which are neonatal rat myoblasts derived from rat hearts. This experiment allows us to detect, visualize, and quantify the protein-protein interaction between RBM20 and Notch2 with high specificity and sensitivity. (Figure 20)
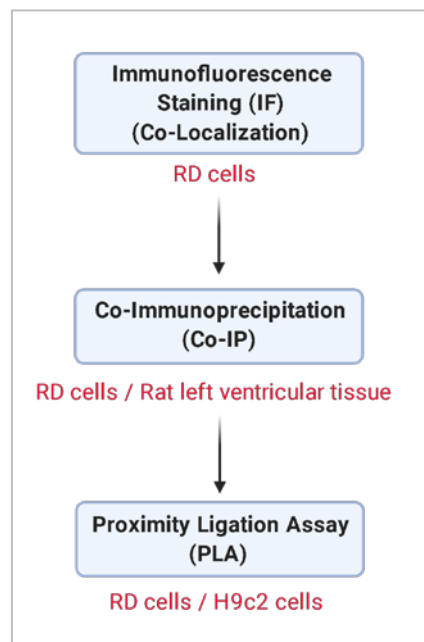
Figure 20 | Experiments planned along with the cell lines and tissues that will be used in each of them.

Moreover, a recent study reported that mutations in the RSRSP stretch of the arginine/serine-rich region of the RBM20 gene disturb the nuclear localization of RBM20 protein, hindering it from translocating to the nucleus and thus diminishing its function [57]. Besides, Notch2 protein was shown to activate the PI3-k/Akt signaling pathway [58], by which RBM20 protein might be phosphorylated, hence activated. Hence, it would be interesting to test the phosphorylation of RBM20 protein by PI3-k,

as well as the amount of phosphorylated / un-phosphorylated RBM20 proteins in Notch2 null mice.

Studying the network of RBM20 interacting partners, and specifically validating its interplay with Notch2 protein will unravel many clues related to the RBM20 protein bio-function and the development of the Dilated Cardiomyopathy phenotype associated with its mutation or deregulation. Advancements in this context will provide novel insights into putative molecular mechanisms responsible for the pathogenesis of DCM. By that time, improved diagnosis and feasible therapeutic modalities for the *RBM20-* associated Dilated Cardiomyopathy will start to emerge.

REFERENCES

1. Guo, W. and M. Sun, *RBM20, a potential target for treatment of cardiomyopathy via titin isoform switching.* Biophysical reviews, 2018. **10**(1): p. 15-25.

2. Lannou, S., et al., *The Public Health Burden of Cardiomyopathies: Insights from a Nationwide Inpatient Study.* Journal of Clinical Medicine, 2020. **9**(4): p. 920.

3. Maron, B.J., et al., *Contemporary definitions and classification of the cardiomyopathies: an American Heart Association scientific statement from the council on clinical cardiology, heart failure and transplantation committee; quality of care and outcomes research and functional genomics and translational biology interdisciplinary working groups; and council on epidemiology and prevention.* Circulation, 2006. **113**(14): p. 1807-1816.

4. Brieler, J., M.A. Breeden, and J. Tucker, *Cardiomyopathy: an overview.* American family physician, 2017. **96**(10): p. 640-646.

5. Paldino, A., et al., *Genetics of dilated cardiomyopathy: clinical implications.* Current cardiology reports, 2018. **20**(10): p. 83.

6. Hershberger, R.E., D.J. Hedges, and A. Morales, *Dilated cardiomyopathy: the complexity of a diverse genetic architecture.* Nature Reviews Cardiology, 2013. **10**(9): p. 531.

7. Maron, B.J., *Hypertrophic cardiomyopathy.* Circulation, 2002. **106**(19): p. 2419-2421.

8. Daughenbaugh, L.A., *Cardiomyopathy: an overview.* The Journal for Nurse Practitioners, 2007. **3**(4): p. 248-258.

9. Muchtar, E., L.A. Blauwet, and M.A. Gertz, *Restrictive cardiomyopathy: genetics, pathogenesis, clinical manifestations, diagnosis, and therapy.* Circulation research, 2017. **121**(7): p. 819-837.

10. Corrado, D., C. Basso, and D.P. Judge, *Arrhythmogenic cardiomyopathy.* Circulation research, 2017. **121**(7): p. 784-802.

11. Pilichou, K., et al., *Arrhythmogenic cardiomyopathy.* Orphanet journal of rare diseases, 2016. **11**(1): p. 33.

12. Corrado, D., M.S. Link, and H. Calkins, *Arrhythmogenic right ventricular cardiomyopathy.* New England journal of medicine, 2017. **376**(1): p. 61-72.

13. Arbustini, E., et al., *Left ventricular noncompaction: a distinct genetic cardiomyopathy?* Journal of the American College of Cardiology, 2016. **68**(9): p. 949-966.

14. Towbin, J.A., *Left ventricular noncompaction cardiomyopathy*, in *Cardioskeletal Myopathies in Children and Young Adults*. 2017, Elsevier. p. 153-171.

15. Oechslin, E. and S. Klaassen, *Left ventricular noncompaction: phenotype in an integrated model of cardiomyopathy?* Journal of the American College of Cardiology, 2019. **73**(13): p. 1612.

16. Zahr, H.C. and D.E. Jaalouk, *Exploring the crosstalk between LMNA and splicing machinery gene mutations in dilated cardiomyopathy.* Frontiers in genetics, 2018. **9**: p. 231.

17. Towbin, J.A., et al., *Incidence, causes, and outcomes of dilated cardiomyopathy in children.* Jama, 2006. **296**(15): p. 1867-1876.

18.	Hänselmann, A., et al., *Dilated cardiomyopathies and non-compaction cardiomyopathy.* Herz, 2020: p. 1-9.

19.	Rosenbaum, A.N., K.E. Agre, and N.L. Pereira, *Genetics of dilated cardiomyopathy: practical implications for heart failure management.* Nature Reviews Cardiology, 2019: p. 1-12.

20.	Weintraub, R.G., C. Semsarian, and P. Macdonald, *Dilated cardiomyopathy.* The Lancet, 2017. **390**(10092): p. 400-414.

21.	Schultheiss, H.-P., et al., *Dilated cardiomyopathy.* Nature Reviews Disease Primers, 2019. **5**(1): p. 1-19.

22.	Pinto, Y.M., et al., *Proposal for a revised definition of dilated cardiomyopathy, hypokinetic non-dilated cardiomyopathy, and its implications for clinical practice: a position statement of the ESC working group on myocardial and pericardial diseases.* European heart journal, 2016. **37**(23): p. 1850-1858.

23.	Pérez-Serra, A., et al., *Genetic basis of dilated cardiomyopathy.* International journal of cardiology, 2016. **224**: p. 461-472.

24.	McNally, E.M., J.R. Golbus, and M.J. Puckelwartz, *Genetic mutations and mechanisms in dilated cardiomyopathy.* The Journal of clinical investigation, 2013. **123**(1): p. 19-26.

25.	van den Hoogenhof, M.M., et al., *RBM20 mutations induce an arrhythmogenic dilated cardiomyopathy related to disturbed calcium handling.* Circulation, 2018. **138**(13): p. 1330-1342.

26.   Watanabe, T., A. Kimura, and H. Kuroyanagi, *Alternative splicing regulator RBM20 and cardiomyopathy.* Frontiers in molecular biosciences, 2018. **5**: p. 105.

27.   Brauch, K.M., et al., *Mutations in ribonucleic acid binding protein gene cause familial dilated cardiomyopathy.* Journal of the American College of Cardiology, 2009. **54**(10): p. 930-941.

28.   Guo, W., et al., *RBM20, a gene for hereditary cardiomyopathy, regulates titin splicing.* Nature medicine, 2012. **18**(5): p. 766.

29.   Zerbino, D., et al., *Giro n CG.* Gil L, Gordon L, Haggerty L, Haskell E, Hourlier T, Izuogu OG, Janacek SH, Juettemann T, To JK, Laird MR, et al, 2018.

30.   Li, D., et al., *Identification of novel mutations in RBM20 in patients with dilated cardiomyopathy.* Clinical and translational science, 2010. **3**(3): p. 90-97.

31.   Refaat, M.M., et al., *Genetic variation in the alternative splicing regulator RBM20 is associated with dilated cardiomyopathy.* Heart Rhythm, 2012. **9**(3): p. 390-396.

32.   Kayvanpour, E., et al., *Genotype-phenotype associations in dilated cardiomyopathy: meta-analysis on more than 8000 individuals.* Clinical Research in Cardiology, 2017. **106**(2): p. 127-139.

33.   Maatz, H., et al., *RNA-binding protein RBM20 represses splicing to orchestrate cardiac pre-mRNA processing.* The Journal of clinical investigation, 2014. **124**(8): p. 3419-3430.

34.   Zhu, C. and W. Guo, *Detection and quantification of the giant protein titin by SDS-agarose gel electrophoresis.* MethodsX, 2017. **4**: p. 320-327.

35. Lahmers, S., et al., *Developmental control of titin isoform expression and passive stiffness in fetal and neonatal myocardium.* Circulation research, 2004. **94**(4): p. 505-513.

36. LeWinter, M.M. and H. Granzier, *Cardiac titin: a multifunctional giant.* Circulation, 2010. **121**(19): p. 2137-2145.

37. Fukuda, N., et al., *Titin isoform variance and length dependence of activation in skinned bovine cardiac muscle.* The Journal of physiology, 2003. **553**(1): p. 147-154.

38. Zhang, T., et al., *The δC isoform of CaMKII is activated in cardiac hypertrophy and induces dilated cardiomyopathy and heart failure.* Circulation research, 2003. **92**(8): p. 912-919.

39. Dzhura, I., et al., *Calmodulin kinase determines calcium-dependent facilitation of L-type calcium channels.* Nature cell biology, 2000. **2**(3): p. 173-177.

40. Beqqali, A., *Alternative splicing in cardiomyopathy.* Biophysical reviews, 2018. **10**(4): p. 1061-1071.

41. George, C.H., et al., *Alternative splicing of ryanodine receptors modulates cardiomyocyte Ca2+ signaling and susceptibility to apoptosis.* Circulation research, 2007. **100**(6): p. 874-883.

42. Mimmi, S., et al., *Phage display: an overview in context to drug discovery.* Trends in pharmacological sciences, 2019. **40**(2): p. 87-91.

43. Marintcheva, B., *Chapter 5 - Phage Display*, in *Harnessing the Power of Viruses*, B. Marintcheva, Editor. 2018, Academic Press. p. 133-160.

44.   Morgan, T.H., *The theory of the gene.* The American Naturalist, 1917. **51**(609): p. 513-544.

45.   Zhou, X. and J. Liu, *Role of Notch signaling in the mammalian heart.* Brazilian Journal of Medical and Biological Research, 2014. **47**(1): p. 1-10.

46.   Hori, K., A. Sen, and S. Artavanis-Tsakonas, *Notch signaling at a glance.* 2013, The Company of Biologists Ltd.

47.   Schwanbeck, R., et al., *The Notch signaling pathway: molecular basis of cell context dependency.* European journal of cell biology, 2011. **90**(6-7): p. 572-581.

48.   Borggrefe, T. and F. Oswald, *The Notch signaling pathway: transcriptional regulation at Notch target genes.* Cellular and molecular life sciences, 2009. **66**(10): p. 1631-1646.

49.   Bray, S.J., *Notch signalling in context.* Nature reviews Molecular cell biology, 2016. **17**(11): p. 722.

50.   Penton, A.L., L.D. Leonard, and N.B. Spinner. *Notch signaling in human development and disease.* in *Seminars in cell & developmental biology.* 2012. Elsevier.

51.   Andersson, E.R., R. Sandberg, and U. Lendahl, *Notch signaling: simplicity in design, versatility in function.* Development, 2011. **138**(17): p. 3593-3612.

52.   MacGrogan, D., J. Münch, and J.L. de la Pompa, *Notch and interacting signalling pathways in cardiac development, disease, and regeneration.* Nature Reviews Cardiology, 2018. **15**(11): p. 685-704.

53.   High, F.A. and J.A. Epstein, *The multifaceted role of Notch in cardiac development and disease.* Nature Reviews Genetics, 2008. **9**(1): p. 49-61.

54.   D'Amato, G., et al., *Sequential Notch activation regulates ventricular chamber development.* Nature cell biology, 2016. **18**(1): p. 7-20.

55.   D'Amato, G., G. Luxán, and J.L. de la Pompa, *Notch signalling in ventricular chamber development and cardiomyopathy.* The FEBS journal, 2016. **283**(23): p. 4223-4237.

56.   Shimizu, K., et al., *Binding of Delta1, Jagged1, and Jagged2 to Notch2 rapidly induces cleavage, nuclear translocation, and hyperphosphorylation of Notch2.* Molecular and Cellular Biology, 2000. **20**(18): p. 6913-6922.

57.   Murayama, R., et al., *Phosphorylation of the RSRSP stretch is critical for splicing regulation by RNA-Binding Motif Protein 20 (RBM20) through nuclear localization.* Scientific reports, 2018. **8**(1): p. 1-14.

58.   Long, J., et al., *JAG2/Notch2 inhibits intervertebral disc degeneration by modulating cell proliferation, apoptosis, and extracellular matrix.* Arthritis research & therapy, 2019. **21**(1): p. 213.